

## RESEARCH ARTICLE SUMMARY

## IMMUNOGENOMICS

# Microglia development follows a stepwise program to regulate brain homeostasis

Orit Matcovitch-Natan,\* Deborah R. Winter,\* Amir Giladi, Stephanie Vargas Aguilar, Amit Spinrad, Sandrine Sarrazin, Hila Ben-Yehuda, Eyal David, Fabiola Zelada González, Pierre Perrin, Hadas Keren-Shaul, Meital Gury, David Lara-Astaiso, Christoph A. Thaiss, Merav Cohen, Keren Bahar Halpern, Kuti Baruch, Aleksandra Deczkowska, Erika Lorenzo-Vivas, Shalev Itzkovitz, Eran Elinav, Michael H. Sieweke,†‡ Michal Schwartz,†‡ Ido Amit†‡

**INTRODUCTION:** Microglia, as the resident myeloid cells of the central nervous system, play an important role in life-long brain maintenance and in pathology. Microglia are derived from erythromyeloid progenitors that migrate to the brain starting at embryonic day 8.5 and continuing until the blood-brain barrier is formed; after this, self-renewal is the only source of new microglia in the healthy brain. As the brain develops, microglia must perform different functions to accommodate temporally changing

needs: first, actively engaging in synapse pruning and neurogenesis, and later, maintaining homeostasis. Although the interactions of microglia with the brain environment at steady state and in response to immune challenges have been well studied, their dynamics during development have not been fully elucidated.

**RATIONALE:** We systematically studied the transcriptional and epigenomic regulation of microglia throughout brain development to

decipher the dynamics of the chromatin state and gene networks governing the transformation from yolk sac progenitor to adult microglia. We used environmental and genetic perturbation models to investigate how timed disruptions to microglia impact their natural development.

**RESULTS:** Global profiles of transcriptional states indicated that microglia development proceeds through three distinct temporal stages, which we define as early microglia (until embryonic day 14), pre-microglia (from embryonic day 14 to a few weeks after birth), and adult microglia (from a few weeks after birth onward).

## ON OUR WEBSITE

Read the full article at <http://dx.doi.org/10.1126/science.aad8670>

ATAC-seq (assay for transposase-accessible chromatin followed by sequencing) for chromatin accessibility and ChIP-seq (chromatin immunoprecipitation followed by sequencing) for histone modifications further characterized the differential regulatory elements in each developmental phase. Single-cell transcriptome analysis revealed minor mixing of the gene expression programs across phases, suggesting that individual cells shift their regulatory networks during development in a coordinated manner. Specific markers and regulatory factors distinguish each phase: For example, we identified *MafB* as an important transcription factor of the adult microglia program. Microglia-specific knockout of *MafB* led to disruption of homeostasis in adulthood and increased expression of interferon and inflammation pathways. We found that microglia from germ-free mice exhibited dysregulation of dozens of genes associated with the adult phase and immune response. In addition, maternal immune activation, which has been linked to behavioral disorders in adult offspring, had the greatest impact on pre-microglia, resulting in a transcriptional shift toward the more advanced developmental stage.

**CONCLUSION:** Our work identifies a stepwise developmental program of microglia in synchrony with the developing brain. Each stage of microglia development has evolved distinct pathways for processing the relevant signals from the environment to balance their time-dependent role in neurogenesis with regulation of immune responses that may cause collateral damage. Genetic or environmental perturbations of these pathways can disrupt stage-specific functions of microglia and lead to loss of brain homeostasis, which may be associated with neurodevelopmental disorders. ■

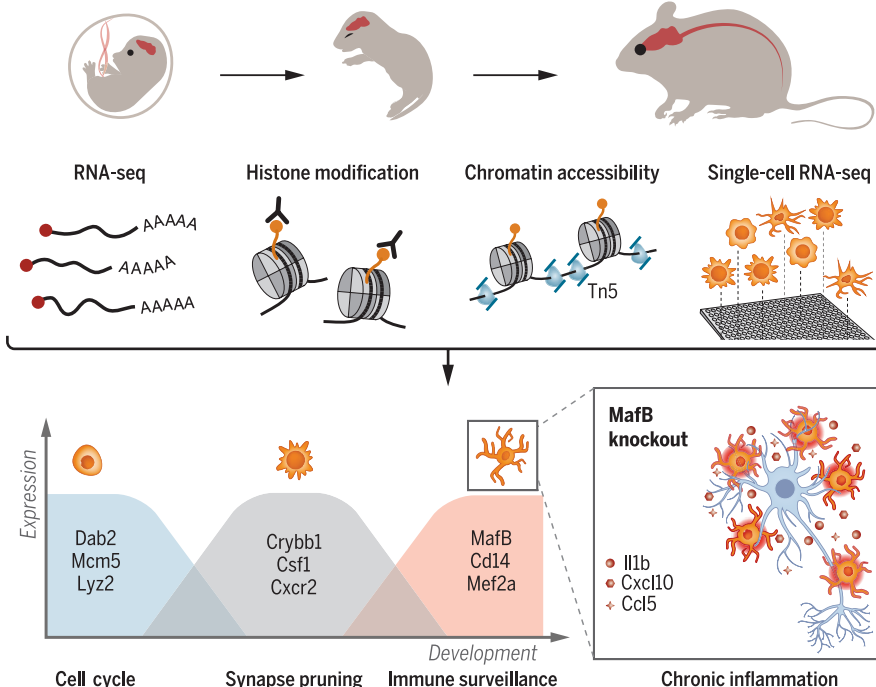
The list of author affiliations is available in the full article online.

\*These authors contributed equally to this work.

†These authors contributed equally to this work.

‡Corresponding author. Email: sieweke@cmi1.univ-mrs.fr (M.H.S.); michal.schwartz@weizmann.ac.il (M.S.); ido.amit@weizmann.ac.il (I.A.)

Cite this article as O. Matcovitch-Natan et al., *Science* **353**, aad8670 (2016). DOI: 10.1126/science.aad8670



**Microglia development proceeds in a stepwise manner.** Microglia were isolated from mice throughout development from embryo to adult. Data from population-level RNA-seq, ChIP-seq, and ATAC-seq, as well as single-cell RNA-seq, show that microglia development proceeds through three distinct stages—early, pre-, and adult—with characteristic gene expression and functional states. Perturbations of this developmental process, such as from *MafB* knockout, lead to disrupted brain homeostasis by the dysregulation of adult and inflammatory genes. Tn5, transposase 5.

## RESEARCH ARTICLE

## IMMUNOGENOMICS

# Microglia development follows a stepwise program to regulate brain homeostasis

Orit Matcovitch-Natan,<sup>1,2\*</sup> Deborah R. Winter,<sup>1\*</sup> Amir Giladi,<sup>1</sup> Stephanie Vargas Aguilar,<sup>3,4,5,6</sup> Amit Spinrad,<sup>1,2</sup> Sandrine Sarrazin,<sup>3,4,5</sup> Hila Ben-Yehuda,<sup>2</sup> Eyal David,<sup>1</sup> Fabiola Zelada González,<sup>3,4,5</sup> Pierre Perrin,<sup>3,4,5</sup> Hadas Keren-Shaul,<sup>1</sup> Meital Gury,<sup>1</sup> David Lara-Astaiso,<sup>1</sup> Christoph A. Thaiss,<sup>1</sup> Merav Cohen,<sup>2</sup> Keren Bahar Halpern,<sup>7</sup> Kuti Baruch,<sup>2</sup> Aleksandra Deczkowska,<sup>2</sup> Erika Lorenzo-Vivas,<sup>1</sup> Shalev Itzkovitz,<sup>7</sup> Eran Elinav,<sup>1</sup> Michael H. Sieweke,<sup>3,4,5,6††</sup> Michal Schwartz,<sup>2,††</sup> Ido Amit<sup>1,††</sup>

**Microglia, the resident myeloid cells of the central nervous system, play important roles in life-long brain maintenance and in pathology. Despite their importance, their regulatory dynamics during brain development have not been fully elucidated. Using genome-wide chromatin and expression profiling coupled with single-cell transcriptomic analysis throughout development, we found that microglia undergo three temporal stages of development in synchrony with the brain—early, pre-, and adult microglia—which are under distinct regulatory circuits. Knockout of the gene encoding the adult microglia transcription factor MAFB and environmental perturbations, such as those affecting the microbiome or prenatal immune activation, led to disruption of developmental genes and immune response pathways. Together, our work identifies a stepwise microglia developmental program integrating immune response pathways that may be associated with several neurodevelopmental disorders.**

**M**icroglia are the resident myeloid cells of the central nervous system (CNS) that control the patterning and wiring of the brain in early development and contribute to homeostasis throughout life (1–3). In the embryo, starting at day 8.5 postconception (E8.5), erythromyeloid progenitors (EMPs) develop in the yolk sac; these cells are CD45<sup>+</sup> cKit<sup>+</sup> and have the capacity to colonize the fetal liver and differentiate into erythrocytes and various myeloid cells, including tissue-resident macrophages (4). A subset of EMPs matures into CX<sub>3</sub>CRI<sup>+</sup> cells in the yolk sac and becomes microglia progenitors (5, 6). These progenitors migrate to the brain starting around days E9.5 to E10.5 and may continue to do so until the formation of the blood-brain

barrier at day E13.5 to E14.5 (4, 7). The microglia population proliferates locally within the brain and distributes spatially in the CNS (8, 9). This original pool of cells is the only source of myeloid cells in the healthy brain (10, 11). Other myeloid cells, such as bone marrow-derived monocytes, only infiltrate the brain under pathological circumstances (6, 12–14).

Myeloid cells, particularly macrophages, are endowed with a higher plasticity than was previously appreciated. They engage in a bidirectional dialogue with their microenvironment, which both shapes their fate and is influenced by their activity (15–18). In the brain, exposure to TGFB1, which acts through the Smad and Irf7 pathways, has been shown to shape the chromatin landscape and influence the response and phenotype of microglia (19, 20). In combination with environmental signals, general lineage-specific factors such as Pu.1 and Irf8 define the microglial regulatory network and distinguish it from other tissue-resident macrophages (7, 15, 16). The evolution of the microglial regulatory network may also be shaped by multiple tissue-specific signals, including protein aggregates, stress signals, and nutrients, as well as the communities of commensal microorganisms colonizing the skin, respiratory, gastrointestinal, and urogenital tract that are collectively termed the microbiota (21, 22). The collection of physiological and pathological cues sensed by microglia, originating from within the brain or externally

(21), may fluctuate spatially across the different brain regions and temporally with development of the brain. Thus, microglial programming must be complex enough to process dynamic environmental signals and execute the temporal functions necessary to accommodate the brain's needs throughout development and adulthood.

It is still unknown how one cell type can have the necessary functional diversity to meet the needs of both the developing brain and life-long maintenance. We hypothesized that microglia acquire specialized functions tailored to changes in the developing brain by a combination of gene regulation and response to environmental signals. Although microglia share many circuits with monocytes, they must maintain tight control of inflammatory and antiviral pathways to prevent neuronal damage, particularly under the various stress conditions that may influence the fetus during pregnancy (23). Thus far, the expression programs and regulatory networks have only been documented for early yolk sac progenitors and adult microglia (2, 7, 15, 16, 19, 24). Microglia modulate synaptic transmission, formation, and elimination and shape embryonic and postnatal brain circuits (25–31). However, many of these processes, such as synaptic pruning and neuronal maturation, peak in mice during the first week after birth—a period that has not previously been profiled in microglia (27–31)—and may be important to understanding the circuits and etiology of many neurodevelopmental diseases.

Perturbation of the microglial environment during development may alter the strict timing of developmental programs, leading to misplaced expression of gene pathways such as inflammation, disrupting neuronal development, and causing brain disorders at later stages in life (30). For example, prenatal exposure to viral infection has been correlated with an increased risk of schizophrenia and autism in mouse and human offspring (32, 33). The precise effects of perturbations on development are highly dependent on the timing of infection, suggesting interference with specific processes (34, 35).

## Results

### Temporal expression profiles during microglia development

To study the dynamics of the gene programs involved in microglia development, we performed RNA sequencing (RNA-seq) to measure the global gene expression of myeloid progenitors from the yolk sac (5) and microglia from embryonic, postnatal, and adult brains (36) for a total of nine time points throughout microglia development (Fig. 1A and fig. S1). Biological replicates were highly correlated ( $r > 0.98$ , Pearson's correlation), and few transcriptional changes were noted across adjacent time points (fig. S2A). Unexpectedly, we found a large number of genes that were differentially expressed across developmental time points (Fig. 1B). Early microglia were associated with genes involved in cell cycling and differentiation, such as *Mcm5* and *Dab2* (37). In contrast, *Csf1*, *Cxcr2*, and other genes involved in neuronal development peaked in expression a

\*Department of Immunology, Weizmann Institute of Science, Rehovot, Israel. <sup>†</sup>Department of Neurobiology, Weizmann Institute of Science, Rehovot, Israel. <sup>‡</sup>Centre d'Immunologie de Marseille-Luminy (CIML), Université Aix-Marseille, UM2, Campus de Luminy, Marseille, France. <sup>§</sup>Institut National de la Santé et de la Recherche Médicale (INSERM), U1104, Marseille, France. <sup>¶</sup>Centre National de la Recherche Scientifique (CNRS), UMR7280, Marseille, France. <sup>||</sup>Max-Delbrück-Centrum für Molekulare Medizin in der Helmholtz-Gemeinschaft (MDC), Robert-Rössle-Strasse 10, 13125 Berlin, Germany.

<sup>††</sup>Department of Cell Biology, Weizmann Institute of Science, Rehovot, Israel.

\*These authors contributed equally to this work. <sup>†</sup>These authors contributed equally to this work. <sup>‡</sup>Corresponding author. Email: sieweke@ciml.univ-mrs.fr (M.H.S.); michal.schwartz@weizmann.ac.il (M.S.); ido.amit@weizmann.ac.il (I.A.)

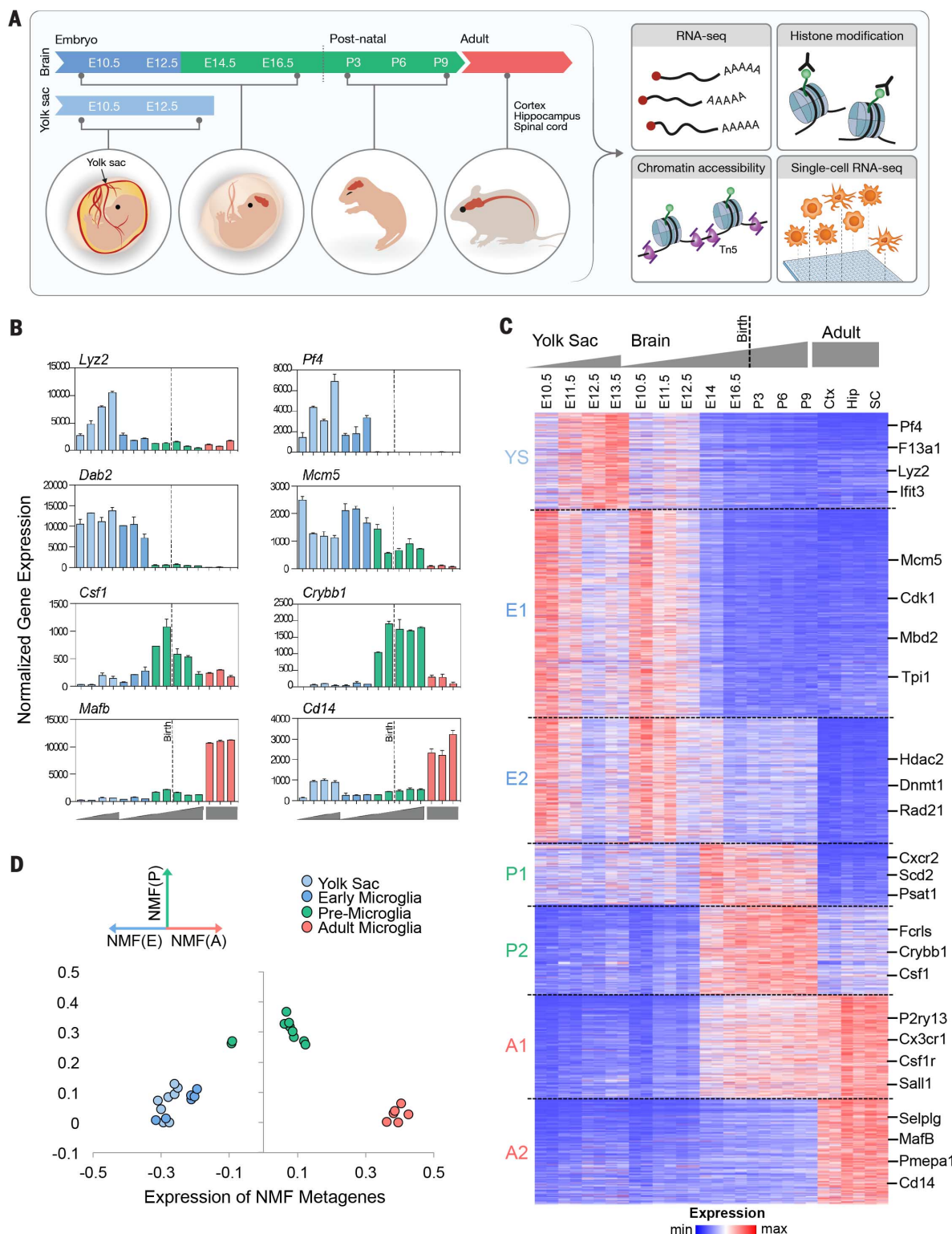


**Fig. 1. Global gene expression patterns reveal distinct microglia developmental phases.** (A) Schematic showing the multidimensional data collected throughout microglia development (Tn5, transposase 5). (B) Bar graphs of expression of a representative set of gene markers across the course of microglia development, as determined by RNA-seq. Error bars indicate SEM. Units on the y axes are arbitrary. Gray polygons below the x axes correspond to the stages shown at the top of (C). (C) K means clustering ( $k = 7$ ) (38) of 3059 genes with differential

expression across the course of microglia development (Ctx, cortex; Hip, hippocampus; SC, spinal cord). Clusters are indicated on the left. (D) NMF analysis of gene expression revealed three metagenes representing distinct transcriptional programs. Samples are color-coded by tissue and program (light blue, yolk sac; blue, early microglia; green, pre-microglia; red, adult microglia). The y axis shows the NMF values for the “pre” metagene (P); the x axis shows the maximum NMF values between the “adult” metagene (A, positive) or the “early” metagene (E, negative).

few days before birth and decreased by adulthood. Canonical adult microglia genes, including *Cd14* and *Pmelal*, were primarily expressed only in adult microglia.

### **Microglia development demonstrates discrete transcriptional phases**

To identify global patterns of gene expression, we performed *k*-means clustering (*k* = 7) that divided the data into four main categories on the basis of the developmental location and timing of gene expression (Fig. 1C; fig. S2, B and C; and table S1). We focused on 3059 of the most highly and differentially expressed genes throughout development (38). We defined these stages as early microglia (1289 genes, clusters E1 and E2, day E10.5 to E14), pre-microglia [589 genes, clusters P1 and P2, day E14 to postnatal day 9 (P9)], and adult microglia (808 genes, clusters A1 and A2, 4 weeks and onward). Adult microglia exhibited only a small number of differentially expressed genes (76 genes; table S2) (38) across different CNS regions including the cortex, hippocampus, and spinal cord. In addition, a group of genes was most highly expressed in the yolk sac (373 genes, cluster YS). Comparison of gene ontologies (GOs) indicated that yolk sac-specific genes were associated with defense response and multiple hematopoietic fates [e.g., *Lyz2* (39) and *Pf4* (40)], whereas shared clusters between the yolk sac and early brain were enriched for genes associated with proliferation and cell cycle (fig. S2B). The yolk sac and early brain microglia showed high correlation at the transcriptional level over time, despite differences in microenvironment (fig. S2A). This observation suggests either that microglia newly arrived to the brain are not immediately adapting upon encountering the neural environment, or alternatively that the first stage of microglia development commences in the yolk sac.

We observed that the pre-microglia stage reflects a distinct phenotype of characteristic genes. Because previous studies have focused on cells from more mature developmental stages, many of these genes have not been annotated with microglia function. However, we found that a subset of the genes that were expressed at this stage was related to the GO categories of neural migration, neurogenesis, and cytokine secretion (fig. S2B). Based on the timing of the pre-microglia program, this phase probably represents when microglia adopt a role in synaptic pruning and neural maturation; later, when the brain matures, they enter a surveillance and homeostatic phase, where they acquire functions associated with tissue maintenance and signaling (41) and express canonical microglia genes (fig. S2B).

To confirm and strengthen the reproducibility of these microglia transcriptional stages, we applied dimension reduction analyses to the RNA-seq data, including nonnegative matrix factorization (NMF) (38, 42) and principal component analysis (PCA). NMF, which deconstructs the data into a given number of metagenes, robustly uncovered three discrete expression programs coinciding with the three microglia stages (Fig. 1D and fig. S2, D to F). Similar results

were obtained with PCA (fig. S1G). This partitioning suggests that the temporal expression profile of microglia development in the brain consists primarily of two major transition events: (i) early microglia to pre-microglia around day E13.5 to E14.5 and (ii) pre-microglia to adult microglia a few weeks after birth.

### **Microglia developmental phases are linked with changes in the chromatin landscape**

The changing chromatin landscape across developmental time points can provide information about the regulatory mechanisms underlying gene expression profiles. Accessible or “open” chromatin regions contain regulatory elements that influence transcription in a cell type–specific or condition-specific manner (43–45). Thus, for each transcriptional stage (yolk sac, early microglia, pre-microglia, and adult microglia), we performed an assay for transposase accessible chromatin followed by sequencing [ATAC-seq (46)] and used a recently developed, highly sensitive method called iChIP (47) for chromatin immunoprecipitation followed by sequencing (ChIP-seq). Unlike what we observed in the RNA-seq data, the chromatin landscape of early microglia was more closely related to that of pre-microglia than to that of the yolk sac stage (fig. S3A), suggesting that chromatin changes precede changes in RNA (47). ATAC-seq identifies accessible regions within promoters (H3K4me3<sup>+</sup> regions near the transcription start site of genes), enhancers [distal regions associated with higher H3K4me1 and -2 (48, 49)], and other regulatory elements, such as CTCF binding sites (46). As observed previously (16), the accessibility of promoter regions was largely conserved over time (fig. S2B). Thus, we focused on candidate enhancers marked by distal ATAC-seq regions with high levels of H3K4me2, as assayed by iChIP (47). These enhancer regions could be divided into four major categories, similar to the gene expression profiles (Fig. 2, A and B; fig. S3, C and D; and table S3). The first category was composed of enhancers marked only in the yolk sac (e.g., F13a1) and may reflect regions that are active in cells not migrating to the brain. A second category comprised enhancers accessible in both the early and pre-microglia, but not in adult microglia. The final two categories consisted of enhancers that are most prominent in adult microglia and are distinguished by whether they are open (e.g., Sall1 and MafB) or closed (e.g., Irf8) earlier in development. Notably, no category was found solely in pre-microglia. This suggests that the pre-microglia phase does not undergo unique chromatin remodeling, but rather exhibits differential usage of the epigenomic landscape established early in microglia development.

To confirm that the observed chromatin changes were related to transitions in microglia development, we assessed whether different enhancer dynamics were associated with the global expression patterns (Figs. 1C and 2B). We linked enhancers to genes by their proximity to the transcription start site (Fig. 2C and table S4) (38). Genomic regions close to genes expressed in the early stage

tended to be in the first two enhancer categories (clusters YS, E1, and E2; Fig. 1C). Similarly, the latter two categories were enriched for genes from the adult microglia transcriptional profile (clusters A1 and A2; Fig. 1C). The dynamics of the microglia enhancer repertoire confirm that the microglia gene expression across developmental stages reflects shifts in the underlying chromatin landscape. However, it is important to note that with bulk data, such as from the RNA expression and chromatin profiling described above, it is unclear whether the transcriptional signal represents the average profile of a heterogeneous mixture of cells from different phases or homogeneous populations where each cell exhibits the relevant temporal profile.

### **Single-cell transcriptome analysis reveals coordinated shifts between phases**

To assess the heterogeneity at each temporal phase in microglia development, we performed massively parallel single-cell RNA-seq [MARS-seq (50)] on a representative time point from each phase. Then we combined the data for cells from all phases and clustered them on the basis of their gene expression profiles (51). To correct for batch effects, each sample was normalized separately before clustering across time points (38). Clustering analysis of 2831 single-cell profiles (696 from the yolk sac stage, 734 from the early microglia stage, 705 from the pre-microglia stage, and 696 from the adult microglia stage) created a detailed map of 2071 differentially expressed genes across 16 transcriptionally homogeneous subpopulations (Fig. 3, A and B). The expression of key marker genes (Fig. 3B and fig. S4A) was combined with global correlation analysis (fig. S4B) to examine the intercluster relationships of transcriptional subpopulations. We determined that each cluster originated almost entirely from a specific stage, confirming that the temporal dynamics of microglia development are the most dominant discriminative feature, even at the single-cell level (Fig. 3C). The exceptions were two subpopulations to which both the yolk sac and early brain time points contributed (VII and VIII; fig. S4C). It is possible that these subpopulations were composed of cells that were on the verge of or had just completed migration to the brain. Moreover, there was additional variation in the yolk sac-specific subpopulation VI and, to a lesser degree, subpopulations II, III, and IV (Fig. 3, A and B, and fig. S4A), which displayed high expression of monocytic genes. When the single-cell subpopulations were compared with the bulk RNA-seq time points (Fig. 1), we found that several of the yolk sac subpopulations (IV to VIII) were best matched to early microglia expression (fig. S4D). This suggests that the yolk sac population is heterogeneous and may include cells with other hematopoietic fates as well as cells with varying levels of commitment to the microglia fate. Once in the brain, their further development occurs in a discrete stepwise fashion that is temporally regulated by environmental cues.

In general, the temporal gene markers that we identified from the bulk RNA-seq analysis exhibited

equivalent expression in the single-cell data (Fig. 3B and fig. S4A). To confirm the stage-specific expression of marker genes (Fig. 3, D to F, upper left panels) in the intact brain, we imaged individual mRNA molecules using single-molecule fluorescent *in situ* hybridization (smFISH) in frozen brain sections from the early, pre-, and adult stages (Fig. 3, D to F, and fig. S5A) (52–54). We found that *Mcm5*, *Csf1*, and *MafB* were en-

riched in CX<sub>3</sub>CRI<sup>+</sup> microglia cells from the early-, pre-, and adult-stage brain, respectively. Immunohistochemistry confirmed that DAB2, a protein that has not been previously associated with microglia, was specifically expressed in early microglia (E12.5), but not at later time points (fig. S5, B and C). Further, *Csf1R* and *Selplg* were expressed in adult microglia, which is consistent with the Allen Brain Atlas (55) (fig. S5D). Taken together, these

results indicate that coordinated transcriptional events control the transitions through microglia development and are probably due to changes in the microenvironment of the CNS.

### Distinct transcription factors regulate microglia developmental phases

Transcription factors play important roles in regulating the chromatin state and gene expression

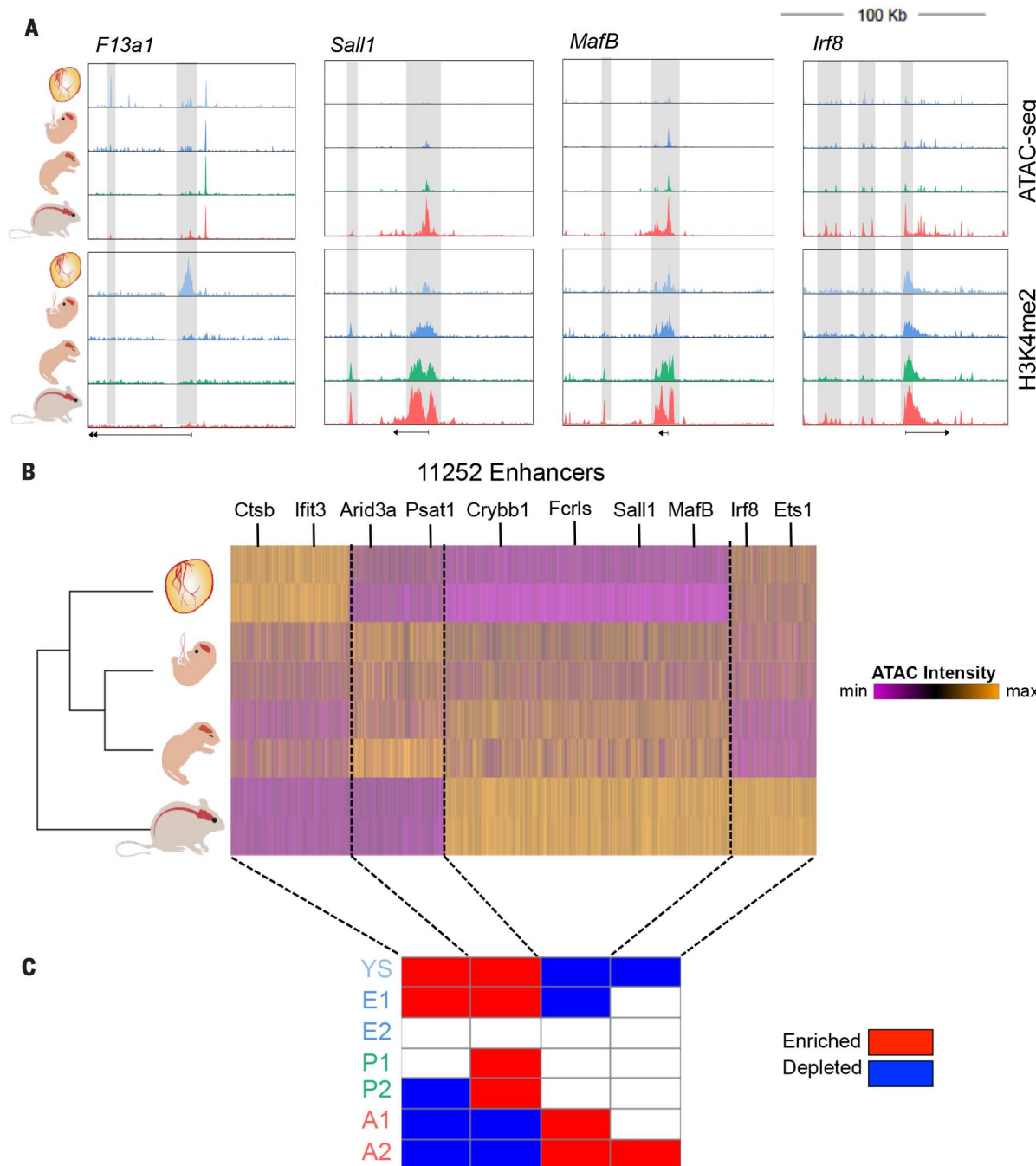


**Fig. 2. Chromatin dynamics reflect distinct phases of microglia development.** (A) Normalized profiles of H3K4me2 and ATAC-seq signals in 100-kilobase (kb) regions from yolk sac progenitors (E12.5; light blue), early microglia (E12.5; blue), pre-microglia (P1; green), and adult microglia (8 weeks; red). Arrows beneath each panel indicate gene location. Gray shading highlights differential chromatin regions. (B) K means clustering ( $k = 4$ ) of ATAC-seq intensity in distal H3 K4me2 regions reveals four main categories of candidate enhancers. (C) Overlap between enhancer dynamics and gene expression clusters from Fig. 1C (boxes marked as enriched or depleted:  $P < 0.05$ , hypergeometric distribution).

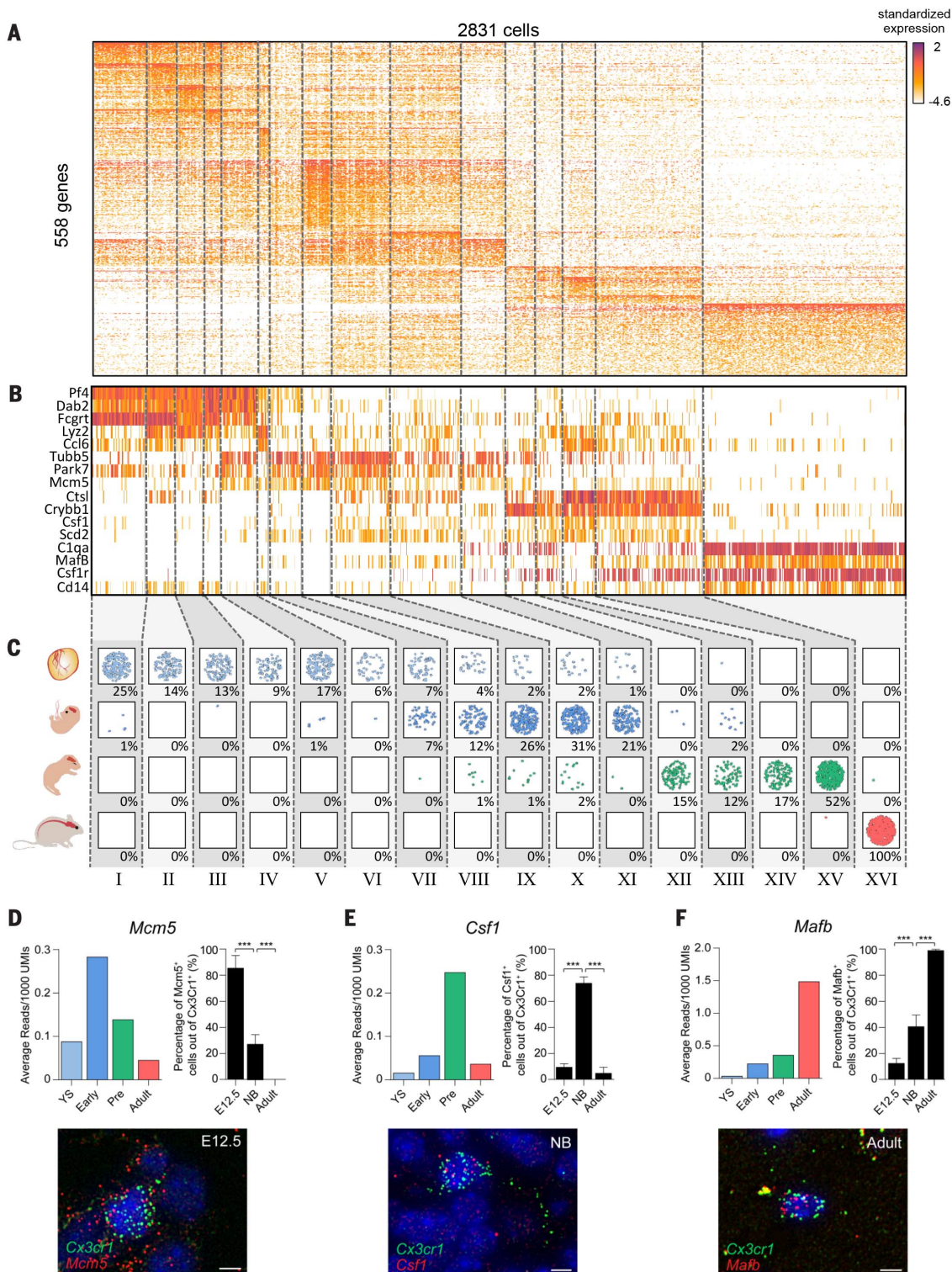


**Fig. 3. Single-cell RNA-seq shows distinct phases of development.** (A) Heatmap showing the 558 most variable genes, organized into clusters ( $k = 16$ ) based on 2071 total differential genes (Materials and methods) in 2831 individual cells isolated from among yolk sac progenitors (E12.5), early microglia (E12.5), pre-microglia (E18.5), and adult microglia (8 weeks). (B) Representative set of marker genes differentially expressed between the different developmental stages. (C) Illustration of the number of sorted cells from each stage (top to bottom: yolk sac, early, pre-, and adult) that were assigned to a given subpopulation defined by the clustering in (A). The percent of cells out of the total in the stage is

given below each box. (D) smFISH of mRNA molecules for *Mcm5*, a marker for early microglia, in intact brain tissue. The top left panel shows the average expression of *Mcm5* across single cells from subpopulations associated with each developmental stage. The top right panel shows the percent of  $\text{CX}_3\text{CR}1^+$  GFP (green fluorescent protein-tagged) cells that overlap *Mcm5* RNA molecules (red). The bottom panel is a representative image of smFISH in an early brain section. (E) Same as (D), but for *Csf1*, a marker for pre-microglia (NB, newborn). (F) Same as (D), but for *Mafb*, a marker for adult microglia. Scale bars, 5  $\mu\text{m}$ . \*\*\* $P < 0.001$ .

of a cell (56, 57). To investigate regulatory factors defining the temporal stages of microglia development, we focused on the expression of genes known to have a DNA binding or chromatin remodeling function and found candidate regulators for each stage (Fig. 4, A and B; fig. S6A; and table S5). In particular, cell cycle factors and chromatin remodelers were highly expressed in the early microglia stage. Canonical microglia transcription factors, such as EGR1 and SALL1, began to be expressed in the pre-microglia stage and were further induced in adulthood. In contrast, we observed several regulators, including JUN, FOS, MEF2A, and MAFB, that were specific to the adult stage and are therefore likely to be involved in establishing microglia homeostatic functions or in terminating developmental functions of pre-microglia (Fig. 4B and fig. S6A).

Motif analysis of the promoters associated with genes from the expression clusters (Fig. 1C) highlighted the differential occurrence of motifs for multiple transcription factors across microglia development (Fig. 4C, fig. S6B, and table S6),

which coincided with the clusters exhibiting the highest expression of the genes encoding these factors. For example, the MEF2A motif was found to be enriched only in the regulatory regions of adult microglia genes. Previous work focusing on the mechanisms of tissue-resident macrophage specification has also suggested that the MEF2 family is important in microglia identity and may play a role in shaping the epigenomic landscape (16). Thus, changes in microglia function throughout development are probably linked to synchronized changes in the underlying regulatory networks.

### MAFB regulates adult microglia homeostasis

We further focused on the functional role of MAFB, one of the principal transcription factors that was highly elevated at the shift from pre- to adult microglia (Figs. 1B, 3B, and 3F). Using immunohistochemistry, we confirmed that MAFB was induced in the transition from pre- to adult microglia (Fig. 5A and fig. S7, A and B). MAFB has previously been shown to be critical for terminal

differentiation of monocytes and tissue-resident macrophages and for restricting their self-renewal capacity (58–60). In addition, the MAF motif has been found to be enriched in macrophage-specific enhancer regions, suggesting that it has the capacity to alter the chromatin landscape in a lineage-specific manner (16). However, the role of MAFB in microglia development and homeostasis has not yet been established.

To address the functional role of MAFB in microglia development, we generated *MafB*<sup>fl/fl</sup>/*Csf1R*<sup>Cre/+</sup> transgenic mice that exhibited loss of *MafB* expression in the macrophage lineage (Fig. 5B and fig. S7, C to E), including microglia, but not in other cells in the CNS. We collected microglia from newborn (pre-microglia) and adult mice and compared their transcriptional profiles with those of control mice (*MafB*<sup>fl/fl</sup>/*Csf1R*<sup>+/+</sup>) of the same age. Successful knockout was confirmed by analyzing *MafB* expression levels (Fig. 5C). Consistent with the strong up-regulation of *MafB* in adult microglia, we observed a greater number of expression changes at the adult stage than at the

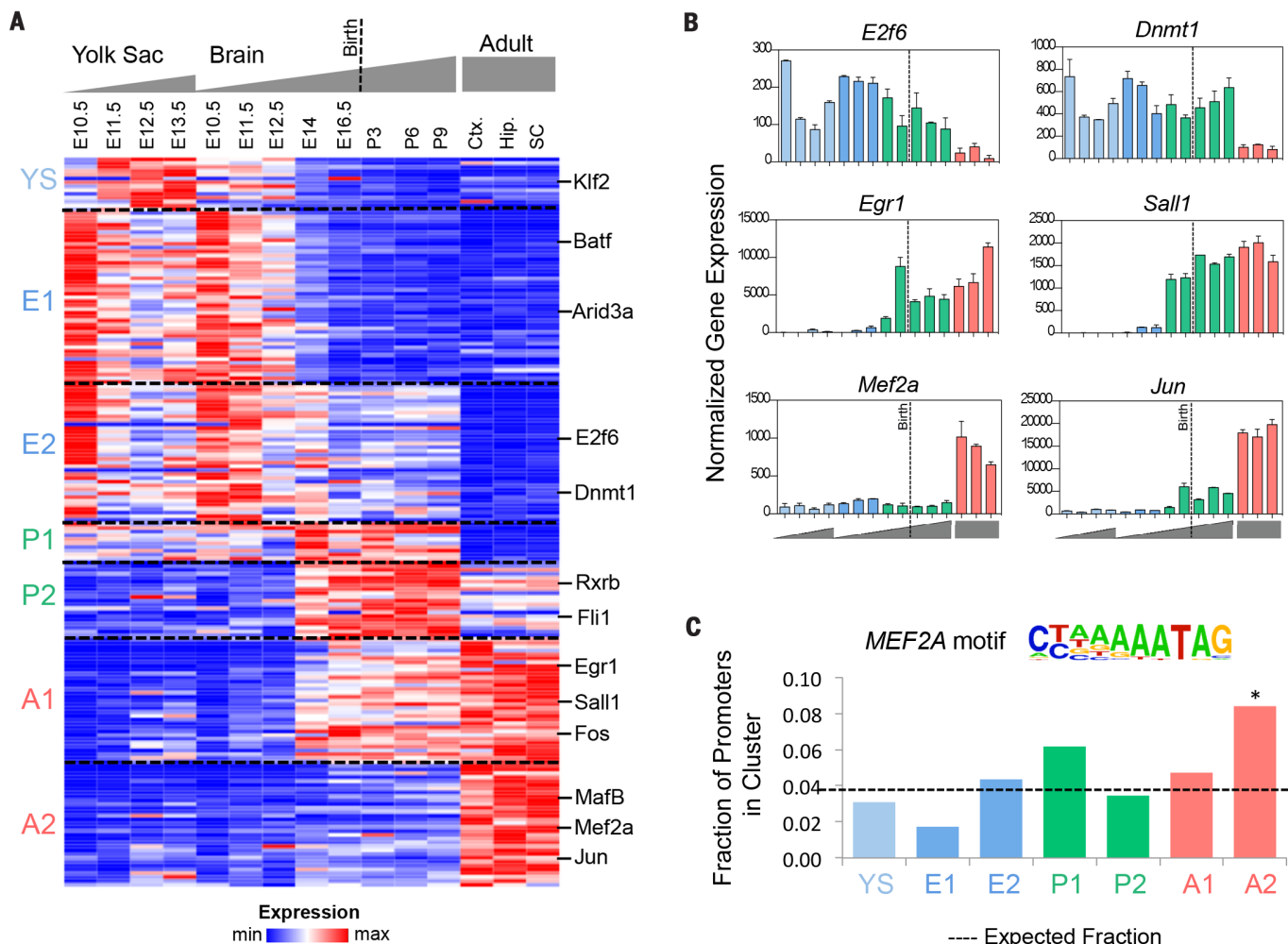


**Fig. 4. Regulatory factors involved in each phase of microglia development.** (A) Heatmap of gene expression of 190 transcription factors and chromatin modifiers from the clusters in Fig. 1C. (B) Bar graphs of expression of representative regulators across microglia development. Error bars indicate SEM. (C) Fraction of promoters associated with genes in each expression cluster (Fig. 1C) containing the sequence motif for MEF2A (logo shown). The dashed line indicates the expected distribution of promoters. \*P < 0.05, hypergeometric distribution, for the significance of enrichment.

pre-microglia stage (Fig. 5, C to E; fig. S7F; and tables S7 and S10). Moreover, all categories of genes regulated by MAFB were significantly enriched for genes expressed in the late adult stage of microglia development, such as *Ctsh* and *Pmepa1* (cluster A2;  $P < 0.05$ , hypergeometric distribution; Fig. 5, C and D, and fig. S7, G and H). Notably, genes that were up-regulated in both pre- and adult microglia included genes in the interferon-STAT pathway, such as *Oas2*, *Mai*, *Ifit3*, *Cacl10*, and *Il1b* (Fig. 5, C and D), and were associated with immune and viral GO terms (fig. S7I). Together, these results

reveal a role for MAFB in suppressing antiviral response pathways and confirm its functional importance in regulating adult microglia homeostasis.

#### Germ-free mice contain microglia with an underdeveloped adult phenotype

To further substantiate the importance of the stepwise microglia development program, we assessed how environmental perturbations in specific stages might differentially affect microglia development and the associated genes. To this end, we chose the models of germ-free (GF) conditions and

maternal immune activation (MIA). Studies have shown that changes in the microbiome affect the immune system as well as the brain (61, 62), and mice with dysbiosis have defects in their microglia population (21). To test whether the microbiome contributes to the environmental signals controlling microglia development, we sorted microglia from GF mice at the pre- (newborn) and adult stages and compared them with those of control mice of the same age housed in a conventional pathogen-free environment. We observed a greater number of genes that were

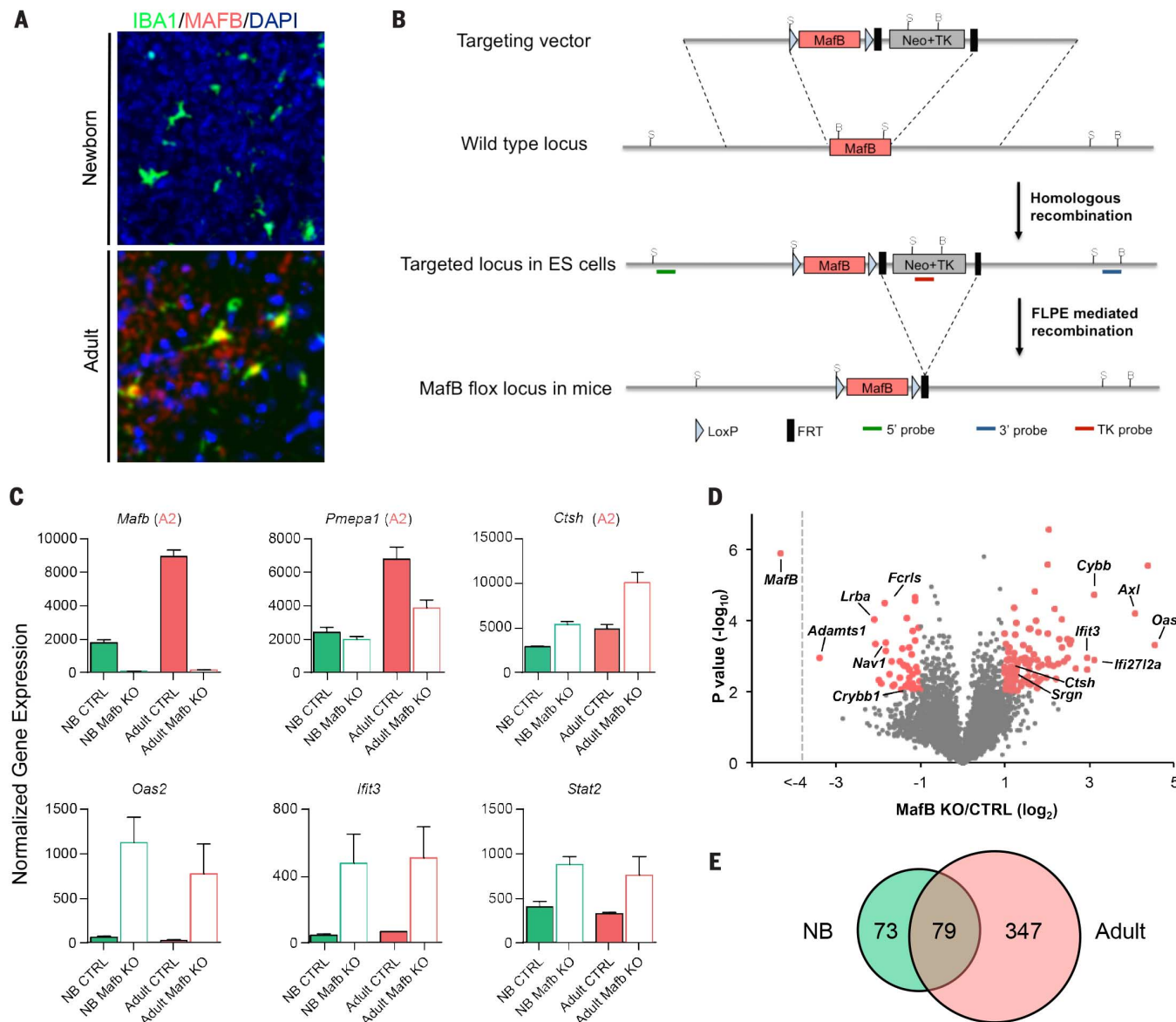


**Fig. 5. MAFB is critical for regulation of homeostasis in adult microglia.**

(A) Representative images of coronal sections from whole brains of mice, showing overlap of immunostaining for Hoechst (blue; DAPI, 4',6-diamidino-2-phenylindole), IBA-1 (green), and MAFB (red) (scale bar, 50  $\mu$ m). Sections taken from adult mice (8 weeks) demonstrate the coexpression of the microglia marker IBA-1 and the protein MAFB, whereas coexpression was not observed in pre-microglia (newborn mice). (B) Diagram of *MafB* knockout mouse generation (Neo, neomycin; TK, thymidine kinase; ES, embryonic

stem cells; FLPE, enhanced Flp recombinase; FRT, flippase recognition target). (C) Expression of representative genes that are dysregulated in either pre- or adult microglia from *MafB* knockout (KO) mice (CTRL, control). Error bars indicate SEM. (D) Volcano plot showing the fold change of genes between *MafB* knockout and control microglia from adult mice on the x axis, with significance of the fold change on the y axis.  $P$  values were determined by a two-tailed  $t$  test. (E) Overlap of differentially regulated genes from pre- (green) and adult (red) microglia.

down-regulated, and down-regulated to a higher degree, in adult microglia compared with those of newborns (322 versus 240) (Fig. 6, A and B; fig. S8, A to C; and tables S8 and S10), which may be explained by the change in microbiome composition at weaning (63, 64). In line with previous reports (21), microglia from GF mice exhibited decreased expression of genes associated with inflammation and defense responses (Fig. 6, B and C, and fig. S8, B and C). Importantly, genes associated with adult microglia (Fig. 6, A and B, and fig. S8C) were also perturbed in adult GF mice: Of the down-regulated developmental genes, a significant fraction were part of the late adult microglia signature (cluster A2, 20 genes;  $P = 1.1 \times 10^{-2}$ , hypergeometric distribution). These results link the microbiome to the transition of microglia from the pre- to adult phenotype and suggest that microglia development is sensitive to perturbations influencing immune signals.

### Microglia development is perturbed by immune activation during pregnancy

MIA by viral infection has been shown to cause neurodevelopmental defects in adult offspring, as well as behavioral deficits (32). Functional abnormalities in the brains of the progeny range from autism to schizophrenia, depending on the timing and conditions of the maternal infection (33). Transient exposure of pregnant mice to polyribonucleic-polyribocytidilic acid (poly I:C) serves as an animal model that reproduces the human disease. Viral infection or poly I:C injection at different stages of the pregnancy leads to distinct neurodevelopmental disease in adulthood, which implicates the specific brain developmental process being executed at the time of intervention (33–35, 65). To examine the effect of MIA on microglia development, we injected pregnant mice with poly I:C at day E14.5 (initiation of the pre-microglia stage) and collected independent samples of mi-

croglia from the newborn and adult offspring of at least two mothers for RNA-seq analysis (fig. S8D and table S9).

In pre-microglia, 174 and 68 developmental genes exhibited at least twofold increased and decreased expression, respectively, in poly I:C offspring compared with phosphate-buffered saline (PBS)-injected controls (Fig. 6, D and E; fig. S8, E and F; and table S10) (38). Within this set, there was significant overlap between genes with increased expression in newborn offspring of mothers injected with poly I:C and those from clusters expressed primarily in adult microglia (clusters A1 and A2; Fig. 1C), whereas depleted genes overlapped with clusters associated with early microglia (clusters E1 and E2; Fig. 1C). Similar results were observed in a comparable experiment with poly I:C injection at E12.5 (fig. S8G). We observed far fewer examples of differential expression in developmental genes at the adult stage compared

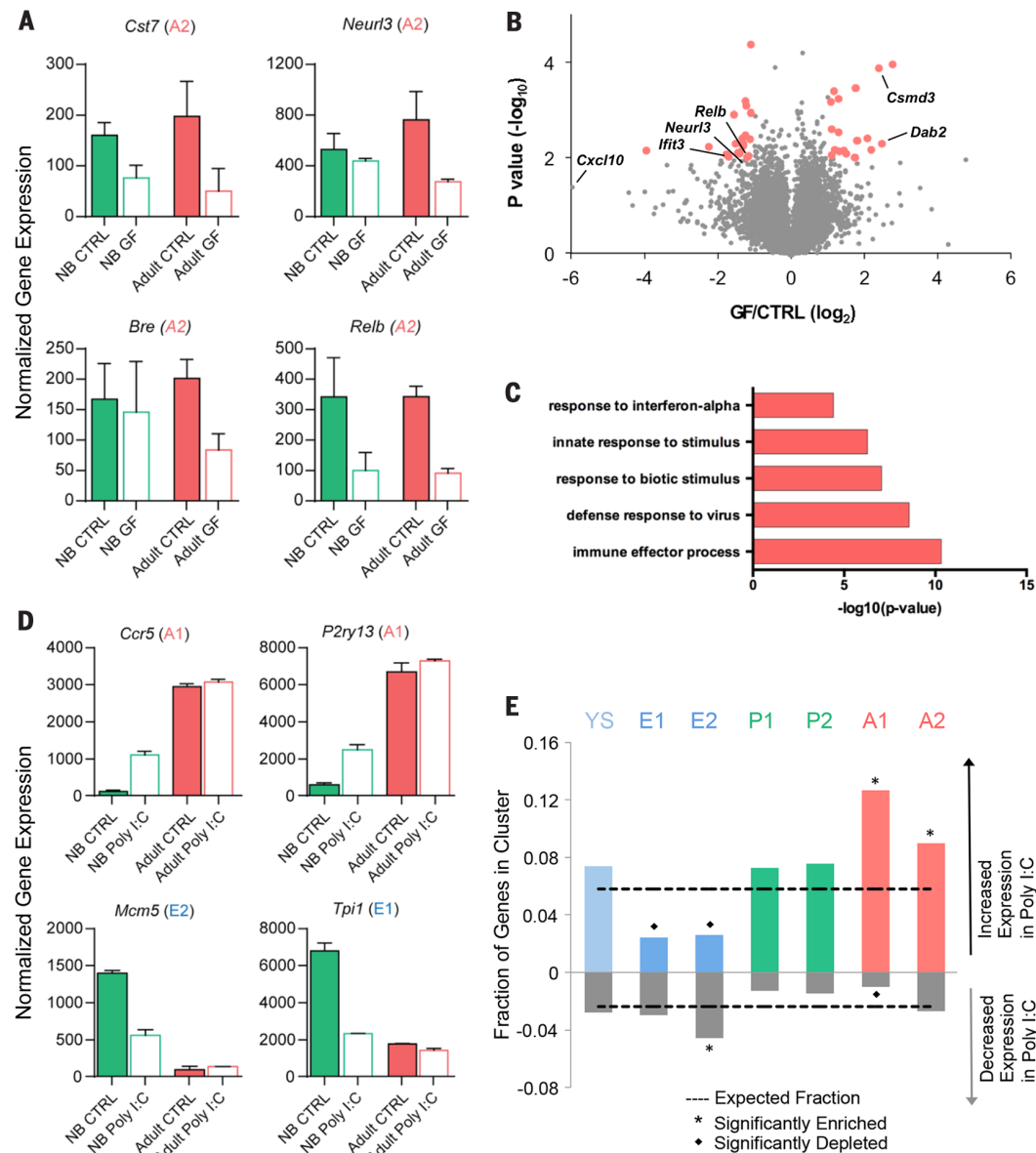


**Fig. 6. Perturbations of immune signals shift microglia expression patterns.** (A) Expression levels in microglia from newborn and adult GF mice compared with those of control mice. Shown are representative genes that are down-regulated in adult microglia. The associated expression cluster from Fig. 1C is indicated. Error bars indicate SEM. (B) Volcano plot showing the fold change between GF and control microglia from adult mice on the x axis, with significance of the fold change on the y axis.  $P$  values were determined by a two-tailed  $t$  test. (C) Enrichment of GO terms in adult down-regulated genes. (D) Expression levels in microglia from newborn and adult offspring of poly I:C-injected (E14.5) mice compared with those from offspring of control mice (PBS-injected). Shown are representative genes that are differentially regulated in pre-microglia. The associated expression cluster from Fig. 1C is indicated. Error bars indicate SEM. (E) Fraction of genes in each expression cluster from Fig. 1C that were differentially regulated (at least a twofold change) in pre-microglia from offspring of poly I:C-injected mice relative to those from offspring of control mice (PBS-injected). The dashed line indicates the expected distribution of genes. \* $P < 0.05$ , hypergeometric distribution, for the significance of enrichment or depletion.

with the pre-microglia stage (fig. S8, E and F), suggesting that the overall expression program of poly I:C mice was realigned with the normal phenotype at adulthood. This may explain why previous studies of adult microglia in MIA did not uncover microglia perturbations (66) and emphasizes that a transient perturbation in microglia development might have far-reaching implications on the brain in adulthood. Overall, microglia from mice subjected to MIA and analyzed at the pre-microglia stage were transcriptionally shifted toward a more advanced developmental stage. We propose that such disruptions in the precise timing of microglia development may perturb their physiological functions in the developing brain and may explain neurodevelopmental diseases in later stages of development, long after the microglia phenotype is restored.

## Discussion

Tissue-resident cells of the immune system must exhibit plasticity in the face of a multitude of signals while still maintaining tight regulation of tissue homeostatic functions. Microglia, as resident myeloid cells in an **immune-privileged** tissue, provide an ideal model for studying the cross-talk of immune cells with the surrounding environment during development. **Once the blood-brain barrier is formed early in development, entry of other immune cells from the periphery is negligible**, so the developmental effects on microglia can be solely attributed to the processes that they undergo within the brain (9, 24). Microglia are not only pivotal during CNS development but are also responsible for brain homeostasis throughout life while restricting deviation such as aggressive inflammation. Here we identify **three distinct phases of regulatory networks in microglia** and demonstrate how perturbation of this tight regulation leads to distinct functional effects.

On the basis of the present findings, we **propose that the expression program of each phase has evolved to support the parallel development of the brain, while keeping in check local innate immune functions that may cause collateral damage**. We might expect to see similar transitions in the resident myeloid cells of other tissues, for example, in Kupffer cells, the resident macrophages of the liver (24, 67). Moreover, resident cells also receive changing signals from their environment as the tissue ages (e.g., increased apoptotic cells); these signals must also be controlled to avoid dangerous responses. Our research highlights the importance of resident myeloid cell adaptation to the changing microenvironment throughout development and the potential for pathologies associated with perturbation of the regulatory circuitry through environmental signals, such as from the microbiome or MIA.

Each stage in microglia development was found to be associated with different signals and functions; thus, the transitions between stages may represent a source of fragility in the system. Perturbations that target these transitions are likely to disrupt different processes depending on the timing and may have an impact on the homeostasis of the adult brain, as indicated by the dysreg-

ulation of the developmental expression patterns of immune response genes. For example, previous research has suggested that the immune system is adapted to natural changes in the microbiota composition related to weaning, which occurs in the first weeks after birth, around the time of the pre- to adult microglia shift (61, 63, 64, 68). **Our results suggest that in mice lacking these microbiome signals, microglia maturity is disrupted with down-regulation of genes associated with inflammation. These signals may reach the brain either directly through certain metabolites (21) or, more likely, indirectly through the effect of systemic immunity on the barriers of the blood-brain interface (69–71)**. On the other hand, a transient MIA at E14.5 has the greatest effect on the pre-microglia stage and is accompanied by an up-regulation of inflammatory genes. Nevertheless, **the resulting behavioral disorders are observed in the offspring at adulthood** and may reflect the impact of the stage-specific microglia response on neurogenesis and synaptic pruning. Such perturbations probably act through distinct regulatory factors in each developmental phase.

**MAFB controls cell cycle arrest** during terminal macrophage differentiation, whereas **its absence is required for macrophage proliferation** (58–60). In this work, we identified the critical influence of MAFB on the ability of microglia to express the adult gene program and its role in inflammatory regulation. Thus, MAFB may represent an important “off-state” factor for regulating the response of microglia under various stress conditions (1). In its absence, dozens of developmental genes are dysregulated, and microglia adopt a dramatic antiviral response state. The role attributed here to MAFB in microglia homeostasis was only detectable in the context of distinct stages of microglia development. The relationship between MAFB and the immune response pathway has yet to be fully described, but previous work suggests that MAFB may have an antagonistic relationship with the interferon pathway (72). This suggests that microglia-specific *MaFB* knockout mice could have an altered interferon response affecting penetrance of neurodevelopmental disease and aging phenotype (69). Further work on MAFB and identification of other signals and factors that contribute to microglia transitions and homeostasis will allow us to better understand the cross-talk between microglia and the CNS in both normal development and pathology.

In light of our results, as well as those emerging with respect to inhibitory factors such as programmed cell death protein 1 (PD-1), it is becoming clear that **the immune system has developed at least as many inhibitory pathways as activating pathways for immune modulation** (73). Further, these immune inhibitory pathways have **probably evolved in a tissue-specific manner to curb immune activation and collateral damage in sensitive tissues such as the brain**. These modulation pathways can be intrinsic (e.g., MAFB) or extrinsic (PD-1) to the cell. A more thorough understanding of the cross-talk between microglia and other cells within the CNS, as well as the signals and pathways that are involved during

development and aging, is essential to developing new approaches for intervention and improved diagnostics.

## Materials and methods

### Animals

*CX<sub>3</sub>CR1*<sup>GFP/+</sup> (74) and wild-type C57/Bl6 mice were taken throughout development as indicated in the text with two replicates at each time point (with the exception of brain E14, which combines samples from E13.5 and E14.5). Timed pregnancy was performed to obtain the embryos at defined time points after conception. Pregnant females with vaginal plugs were determined as 0.5 dpc. Adult mice were taken at 8 weeks. Animals were supplied by the Animal Breeding Center of the Weizmann Institute of Science. All animals were handled according to the regulations formulated by the Institutional Animal Care and Use Committee.

### Isolation of hematopoietic cells from yolk sacs

Yolk sacs were dissected from staged embryos. Single-cell suspensions were achieved using a software-controlled sealed homogenization system (Dispomix; [www.biocellisolation.com](http://www.biocellisolation.com)) in PBS. Cell suspensions were first blocked with Fc-block CD16/32 (BD Biosciences, San Jose, CA), and then stained for CD45<sup>+</sup> (1:150; 30-F11, BioLegend, San Diego, CA), CD11b<sup>+</sup> (1:150; M1/70, BioLegend, San Diego, CA) and gated for CX<sub>3</sub>CR1-GFP positive. Cell populations were sorted with SORP-aria.

### Microglia harvesting

Naïve C57BL/6J female mice were bred overnight with CX<sub>3</sub>CR1<sup>GFP/GFP</sup> males (74). Vaginal plugs were checked the next morning and were referred to as embryonic day 0.5 (E0.5). Mice were taken at different time points as indicated in the text; adult mice cortex, hippocampus, and spinal cords were taken at age of 8 weeks. Prenatal brains were dissected and stripped of meninges. Adult and postnatal mice were perfused with PBS transcardially; brains were dissected and stripped of meninges and choroid plexus. Single-cell suspensions were achieved using a software-controlled sealed homogenization system (Dispomix; [www.biocellisolation.com](http://www.biocellisolation.com)) in PBS, followed by density gradient separation; pellet was mixed with 40% percoll and centrifuged at 800g for 20 min at room temperature. Supernatant was discarded and pellet taken further for antibody staining. Samples were first blocked with Fc-block CD16/32 (BD Biosciences, San Jose, CA) and then gated for CD45<sup>int</sup> (1:150; 30-F11, BioLegend), CD11b<sup>int</sup> (1:150; M1/70, BioLegend), and CX<sub>3</sub>CR1-GFP<sup>+</sup>. Cell populations were sorted with SORP-aria (BD Biosciences, San Jose, CA).

### Germ-free mice

Wild-type C57/Bl6 mice were born and raised in sterile isolators in the absence of any microbial colonization as described previously (75). Sterility was routinely monitored by PCR- and culture-based methods. Brains from GF mice and SPF controls were taken at day 1 and week 4. Microglia

from whole brains were harvested as described above and gated for CD45<sup>int</sup> and CD11b<sup>int</sup>, as we and others have carefully confirmed these cells to be similar to the populations collected from the CX<sub>3</sub>CRI-GFP<sup>+</sup> microglia populations (see fig. S1C). Cell populations were sorted with SORP-aria (BD Biosciences, San Jose, CA).

### Maternal immune activation by poly I:C

Naïve female mice were bred overnight with C57BL/6J males. Vaginal plugs were checked the next morning and were referred to as embryonic day 0.5 (E0.5). On E12.5 or E14.5, pregnant females were injected intravenously (i.v.) with a single dose of 5 mg/kg poly I:C (Sigma-Aldrich, Rehovot, Israel) dissolved in PBS, or an equivalent volume of PBS as a control. The dose of poly I:C was determined according to Meyer *et al.* (76). The injection volume was 5 ml/kg. Pups from injected animals were taken at postnatal day 1 and at age of 4 weeks. Microglia were harvested from whole brains as described above, and gated by CD45<sup>int</sup> and CD11b<sup>int</sup>, as we and others have carefully confirmed these cells to be similar to the populations collected from the CX<sub>3</sub>CRI-GFP<sup>+</sup> microglia populations (see fig. S1C). Cell populations were sorted with SORP-aria (BD Biosciences, San Jose, CA).

### MafB knockout mice

Female MafB<sup>flox/+</sup>Csf1R<sup>+/+</sup> or MafB<sup>flox/flox</sup>Csf1RCre<sup>+/+</sup> were bred with male MafB<sup>flox/flox</sup>Csf1R-Cre<sup>Cre/+</sup> (refer to the supplementary materials for description of knockout generation). Vaginal plugs were checked the next morning and were referred to as embryonic day 0.5 (E0.5). Postnatal mice were taken at P2 and adults at age of 5 weeks; animals were perfused with PBS transcardially; brains were dissected and stripped of meninges and choroid plexus. Microglia were harvested from whole brains. Single-cell suspension was achieved by mechanical dissociation, followed by density gradient separation; pellet was mixed with 70% percoll and overlayed on 37% percoll underlaid by 30% percoll, centrifuged at 800g for 30 min at 4°C. 37%/70% interface was collected for antibody staining. Samples were pre-gated using Zombie Violet fixable viability kit (BioLegend, France) and Ly6C<sup>-</sup> (HK1.4, BioLegend, France) and then gated for CD45.2<sup>int</sup> (104, BD Biosciences, France) and CD11b<sup>int</sup> (1:150; M1/70, BD Biosciences, France). Cell populations were sorted with SORP-ariaBD FACS Aria III (BD Biosciences, France).

### Single-molecule fluorescent *in situ* hybridization

CX<sub>3</sub>CRI-GFP<sup>+</sup> were perfused, brain tissues were harvested and fixed in 4% paraformaldehyde for 3 hours, incubated overnight with 30% sucrose in 4% paraformaldehyde, and then embedded in OCT. 7-μm cryosections were used for hybridization. Probe libraries were designed and constructed as previously described (53). Single-molecule FISH probe libraries consisted of 48 probes of length 20 bps and were coupled to cy5 or alexa594. Hybridizations were performed overnight in 30°C. DAPI dye for nuclear staining was added during

the washes. To detect microglia, CX<sub>3</sub>CRI-GFP<sup>+</sup> mice were used and cells were detected by their GFP fluorescent signal. Images were taken with a Nikon Ti-E inverted fluorescence microscope equipped with a ×100 oil-immersion objective and a Photometrics Pixis 1024 charge-coupled device camera using MetaMorph software (Molecular Devices, Downingtown, PA). The image-plane pixel dimension was 0.13 μm. *P* values were calculated by Fisher exact test (77).

### RNA sequencing

Cells were harvested at different time points into Lysis/Binding buffer (Invitrogen). mRNA was captured with 12 μl of Dynabeads oli-go(dT) (Life Technologies), washed, and eluted at 70°C with 10 μl of 10 mM Tris-Cl (pH 7.5). RNA-seq was performed as previously described (50), and DNA libraries were sequenced on an Illumina NextSeq 500 or HiSeq with an average of 4 million aligned reads per sample.

### RNA processing and analysis

We aligned the RNA-seq reads to the mouse reference genome (NCBI 37, mm9) using TopHat v2.0.13 with default parameters (78). Duplicate reads were filtered if they aligned to the same base and had identical UMIs. Expression levels were calculated and normalized for each sample to the total number of reads using HOMER software (<http://homer.salk.edu>) with the command “analyzeRepeats.pl rna mm9 -d [sample files] -count 3utr -condenseGenes” (79). For the RNA-seq analysis in Fig. 1, we focused on highly expressed genes with twofold differential over the noise (set at 100) between the means of at least two time points (3059 genes). The value of *k* for the *k* means clustering (Matlab function *kmeans*) was chosen by assessing the average silhouette (Matlab function *evalclusters*; higher score means more cohesive clusters) for a range of possible values with correlation as the distance metric (fig. S1C). GO associations for each cluster were determined using GOrilla (<http://cbl-gorilla.cs.technion.ac.il/>) (80, 81). The overlap with microglia-specific genes was determined by comparison with genes from the brain-specific macrophage expression cluster in (16) and the significance of enrichment was calculated using a hypergeometric distribution. The subset of genes that were differential across CNS regions was determined based on a greater than twofold differential between any two of the three regions (cortex, hippocampus, and spinal cord) and the highest expression of the three falling within twofold of the maximum expression across microglia development. NMF and PCA were performed using built-in Matlab functions *nnmf* and *pca*, respectively. The value of *k* for the NMF was chosen by assessing the plot of root mean square residuals for a range of values (fig. S1F).

### iChIP

Naïve C57BL/6J female mice were bred overnight with CX<sub>3</sub>CRI-GFP/GFP males (74). Vaginal plugs were checked the next morning and were referred to as embryonic day 0.5 (E0.5). Mice were taken at

E12.5, day 1, and 8 weeks. Microglia were harvested from whole brains and sorted as indicated above. iChIP was prepared as previously described (47).

### ATAC-seq

Naïve C57BL/6J female mice were bred overnight with CX<sub>3</sub>CRI-GFP/GFP males (74). Vaginal plugs were checked the next morning and were referred to as embryonic day 0.5 (E0.5). Mice were taken at E12.5, day 3, and 8 weeks. Microglia were harvested from whole brains and sorted as indicated above. To profile for open chromatin, we used an adaptation of the ATAC-seq protocol (46, 82) as previously described (16).

### Processing of ChIP-seq and ATAC-seq

Reads were aligned to the mouse reference genome (mm9, NCBI 37) using Bowtie2 aligner version 2.2.5 (83) with default parameters. The Picard tool *MarkDuplicates* from the Broad Institute (<http://broadinstitute.github.io/picard/>) was used to remove PCR duplicates. To identify regions of enrichment (peaks) from ChIP-seq reads of H3K4me2 and ATAC-seq, we used the HOMER package *makeTagDirectory* followed by *findPeaks* command with the histone parameter or 500-bp centered regions, respectively (79). Union peaks file were generated for ATAC by combining and merging overlapping peaks in all samples.

### Chromatin analysis

The read density (number of reads in 10 million total reads per 1000 bp) for H3K4me2 and ATAC was calculated in each region from the union ATAC peaks files. We consider promoters to be within ± 2000 bp of a TSS (*n* = 12930). We defined 11,252 high-confidence distal enhancers based on their presence in at least two replicates of the same ATAC-seq population, the distal location of the regions (i.e., excluding promoters), and the average H3 K4me2 read density. The region intensity was given in log-base2 of the normalized density [ $\log_2(x + 1)$ ]. The value of *k* for the *k*-means clustering (Matlab function *kmeans*) was chosen by assessing the average silhouette (Matlab function *evalclusters*) for a range of possible values with correlation as the distance metric (fig. S3D). The significance of the overlap between chromatin categories and expression clusters was determined using the hypergeometric distribution (*P* < 0.05; table S4).

### Gene tracks and normalization

All gene tracks were visualized as *bigWig* files of the combined replicates normalized to 10,000,000 reads and created by the HOMER algorithm *makeUCSCfile* (79). For visualization, the tracks were smoothed by averaging over a sliding window of 500 bases and all tracks for a given region were scaled to the highest overall peak.

### Single-cell sorting

Naïve C57BL/6J female mice were bred overnight with CX<sub>3</sub>CRI-GFP/GFP males (74). Vaginal plugs were checked the next morning and were referred to as embryonic day 0.5 (E0.5). Mice

were taken at E12.5, E18.5, and 8 weeks. Microglia were harvested and sorted from whole brains as indicated above into 384-well cell capture plates containing 2 µl of lysis solution and barcoded poly(T) reverse-transcription (RT) primers for single-cell RNA-seq (50). Barcoded single-cell capture plates were prepared with a Bravo automated liquid handling platform (Agilent) as described previously (50). Four empty wells were kept in each 384-well plate as a no-cell control during data analysis. Immediately after sorting, each plate was spun down to ensure cell immersion into the lysis solution, snap frozen on dry ice, and stored at -80°C until processed.

### Single-cell libraries and analysis

Single-cell libraries were prepared using the MARS-seq protocol and processed as described previously (50). In order to assess the heterogeneity of the previously defined phases in microglia development, we used a recently published batch-aware multinomial mixture-model clustering algorithm (51). Since samples derive from different spatial and temporal points, we devised an approach that would reduce batch effect within each sample but preserve genuine gene expression differences between samples. Each sample, consisting of four batches, was clustered separately. This preliminary clustering was used to infer optimum batch correction coefficients for each gene. A new debatched UMI data set was created, implementing the inferred corrections on the UMI count. The debatched data set was then used to jointly cluster all samples using the same algorithm with no debatching (all batch correction coefficients were set to 1).

This two-step clustering approach proved to increase likelihood score and significantly reduce intra-cluster gene variance when compared with clustering each sample separately, allowing debatching between samples or disallowing debatching completely.

### Immunohistochemistry

Mice were transcardially perfused with PBS before brain tissue fixation. The following primary antibodies were used: mouse anti-Dab2 (1:100; BD Bioscience, San Jose, CA), Rabbit anti-GFP (1:100; MBL, Woburn, MA), Goat anti-GFP (1:100; Abcam, Cambridge, MA), Goat anti-IBA1 (1:100; Abcam, Cambridge, MA), Rabbit anti-MAFB (1:100; Bethyl Laboratories, Montgomery, TX). Secondary antibodies were Cy3/Cy2 conjugated donkey anti-mouse/goat antibodies (1:200; Jackson ImmunoResearch, West Grove, PA). The slides were exposed to Hoechst nuclear staining (1:4000; Invitrogen Probes, Carlsbad, CA) for 1 min before their sealing. Two negative controls were used in immunostaining procedures: staining with isotype control antibody followed by secondary antibody, or staining with secondary antibody alone.

For DAB2 staining, microglia from CX<sub>3</sub>CR1<sup>GFP/+</sup> mice underwent tissue processing and immunohistochemistry on paraffin embedded sectioned (6 µm thick). Microscopic analysis was performed using a fluorescence microscope (E800; Nikon).

For MAFB staining, microglia from wild-type mice underwent tissue processing and immunohistochemistry on floating sections (30 µm thick). Microscopic analysis was performed using confocal microscopy (Zeiss, LSM880).

### Motif analysis

For motif finding, we used the sets of genes from each expression cluster (Fig. 1C) individually as input for the HOMER package motif finder algorithm *findMotifGenome.pl* (79). By parsing the known motif list, we compiled the occurrences of the sequence motifs for the transcription factors of interest within the promoters of each expression cluster. A hypergeometric distribution was used to calculate the significance of the overlap between motif occurrences in our set and the expression clusters from Fig. 1C.

### Statistical methods

In general, two replicates (in some cases, averaged over offspring from same mother) per sample from independent mice were used for the analyses, so that expression differences would be comparable between time points. In the poly I:C experiment, replicates originated from different mothers. The *MaFb* knockout experiment used three replicates from independent mice for both newborn and adult. Genes were considered to have increased or decreased in expression if the log fold change was greater than 1 between the mean of replicates. Genes with normalized log expression value less than 6 were not used for this comparison because of the noise at these low expression levels. *P* values for expression changes used in the volcano plots were calculated using a two-tailed *t* test on the log expression values. A hypergeometric distribution was used to calculate the significance of the overlap between differentially expressed genes, motifs, chromatin clusters, and the expression clusters from Fig. 1C. GO associations and related *P* values were determined using GOrilla (<http://cbl-gorilla.cs.technion.ac.il/>) (80, 81). Pairwise similarity between replicates or samples was given as the Pearson's correlation.

Further details are included in the supplementary materials.

### REFERENCES AND NOTES

- U.-K. Hanisch, H. Kettenmann, Microglia: Active sensor and versatile effector cells in the normal and pathologic brain. *Nat. Neurosci.* **10**, 1387–1394 (2007). doi: [10.1038/nrn1997](https://doi.org/10.1038/nrn1997); pmid: [17965659](https://pubmed.ncbi.nlm.nih.gov/17965659/)
- A. Nimmerjahn, F. Kirchhoff, F. Helmchen, Resting microglial cells are highly dynamic surveillants of brain parenchyma in vivo. *Science* **308**, 1314–1318 (2005). doi: [10.1126/science.1110647](https://doi.org/10.1126/science.1110647); pmid: [15831717](https://pubmed.ncbi.nlm.nih.gov/16030000/)
- M. Prinz, J. Priller, S. S. Sisodia, R. M. Ransohoff, Heterogeneity of CNS myeloid cells and their roles in neurodegeneration. *Nat. Neurosci.* **14**, 1227–1235 (2011). doi: [10.1038/nn.2923](https://doi.org/10.1038/nn.2923); pmid: [21952260](https://pubmed.ncbi.nlm.nih.gov/21952260/)
- E. Gomez Perdiguero et al., Tissue-resident macrophages originate from yolk-sac-derived erythro-myeloid progenitors. *Nature* **518**, 547–551 (2015). doi: [10.1038/nature13989](https://doi.org/10.1038/nature13989); pmid: [25470051](https://pubmed.ncbi.nlm.nih.gov/25470051/)
- F. Ginhoux et al., Fate mapping analysis reveals that adult microglia derive from primitive macrophages. *Science* **330**, 841–845 (2010). doi: [10.1126/science.1194637](https://doi.org/10.1126/science.1194637); pmid: [20966214](https://pubmed.ncbi.nlm.nih.gov/20966214/)
- C. Schulz et al., A lineage of myeloid cells independent of Myb and hematopoietic stem cells. *Science* **336**, 86–90 (2012). doi: [10.1126/science.1219179](https://doi.org/10.1126/science.1219179); pmid: [22442348](https://pubmed.ncbi.nlm.nih.gov/22442348/)
- K. Kierdorf et al., Microglia emerge from erythromyeloid precursors via Pu.1- and Irf8-dependent pathways. *Nat. Neurosci.* **16**, 273–280 (2013). doi: [2334579](https://doi.org/10.1038/nn.3457)
- J. Bruttger et al., Genetic cell ablation reveals clusters of local self-renewing microglia in the mammalian central nervous system. *Immunity* **43**, 92–106 (2015). doi: [10.1016/j.jimmuni.2015.06.012](https://doi.org/10.1016/j.jimmuni.2015.06.012); pmid: [26163371](https://pubmed.ncbi.nlm.nih.gov/26163371/)
- B. Ajami, J. L. Bennett, C. Krieger, W. Tetzlaff, F. M. V. Rossi, Local self-renewal can sustain CNS microglia maintenance and function throughout adult life. *Nat. Neurosci.* **10**, 1538–1543 (2007). doi: [10.1038/nn2014](https://doi.org/10.1038/nn2014); pmid: [1802609](https://pubmed.ncbi.nlm.nih.gov/17802609/)
- D. Hashimoto et al., Tissue-resident macrophages self-maintain locally throughout adult life with minimal contribution from circulating monocytes. *Immunity* **38**, 792–804 (2013). doi: [10.1016/j.jimmuni.2013.04.004](https://doi.org/10.1016/j.jimmuni.2013.04.004); pmid: [23601688](https://pubmed.ncbi.nlm.nih.gov/23601688/)
- J. Sheng, C. Ruehl, K. Karjalainen, Most tissue-resident macrophages except microglia are derived from fetal hematopoietic stem cells. *Immunity* **43**, 382–393 (2015). doi: [10.1016/j.jimmuni.2015.07.016](https://doi.org/10.1016/j.jimmuni.2015.07.016); pmid: [26287683](https://pubmed.ncbi.nlm.nih.gov/26287683/)
- A. Mildner et al., Microglia in the adult brain arise from Ly-6Ch<sup>CCR2+</sup> monocytes only under defined host conditions. *Nat. Neurosci.* **10**, 1544–1553 (2007). doi: [10.1038/nn2015](https://doi.org/10.1038/nn2015); pmid: [18026096](https://pubmed.ncbi.nlm.nih.gov/18026096/)
- R. Schechter et al., Infiltrating blood-derived macrophages are vital cells playing an anti-inflammatory role in recovery from spinal cord injury in mice. *PLOS Med.* **6**, e1000113 (2009). doi: [10.1371/journal.pmed.1000113](https://doi.org/10.1371/journal.pmed.1000113); pmid: [19636355](https://pubmed.ncbi.nlm.nih.gov/19636355/)
- R. Schechter et al., Recruitment of beneficial M2 macrophages to injured spinal cord is orchestrated by remote brain choroid plexus. *Immunity* **38**, 555–569 (2013). pmid: [23477737](https://pubmed.ncbi.nlm.nih.gov/23477737/)
- D. Gosselin et al., Environment drives selection and function of enhancers controlling tissue-specific macrophage identities. *Cell* **159**, 1327–1340 (2014). doi: [10.1016/j.cell.2014.11.023](https://doi.org/10.1016/j.cell.2014.11.023); pmid: [25480297](https://pubmed.ncbi.nlm.nih.gov/25480297/)
- Y. Lavin et al., Tissue-resident macrophage enhancer landscapes are shaped by the local microenvironment. *Cell* **159**, 1312–1326 (2014). doi: [10.1016/j.cell.2014.11.018](https://doi.org/10.1016/j.cell.2014.11.018); pmid: [25480296](https://pubmed.ncbi.nlm.nih.gov/25480296/)
- M. Greter et al., Stroma-derived interleukin-34 controls the development and maintenance of Langerhans cells and the maintenance of microglia. *Immunity* **37**, 1050–1060 (2012). doi: [10.1016/j.jimmuni.2012.11.001](https://doi.org/10.1016/j.jimmuni.2012.11.001); pmid: [23177320](https://pubmed.ncbi.nlm.nih.gov/23177320/)
- Y. Wang et al., IL-34 is a tissue-restricted ligand of CSFR required for the development of Langerhans cells and microglia. *Nat. Immunol.* **13**, 753–760 (2012). doi: [10.1038/ni.2360](https://doi.org/10.1038/ni.2360); pmid: [22729249](https://pubmed.ncbi.nlm.nih.gov/22729249/)
- O. Butovsky et al., Identification of a unique TGF-β-dependent molecular and functional signature in microglia. *Nat. Neurosci.* **17**, 131–143 (2014). doi: [10.1038/nn.3599](https://doi.org/10.1038/nn.3599); pmid: [24316888](https://pubmed.ncbi.nlm.nih.gov/24316888/)
- M. Cohen et al., Chronic exposure to TGFβ1 regulates myeloid cell inflammatory response in an IRF7-dependent manner. *EMBO J.* **33**, 2906–2921 (2014). doi: [10.15252/embj.201489293](https://doi.org/10.15252/embj.201489293); pmid: [25385836](https://pubmed.ncbi.nlm.nih.gov/25385836/)
- D. Erny et al., Host microbiota constantly control maturation and function of microglia in the CNS. *Nat. Neurosci.* **18**, 965–977 (2015). doi: [10.1038/nn.4030](https://doi.org/10.1038/nn.4030); pmid: [26030851](https://pubmed.ncbi.nlm.nih.gov/26030851/)
- S. Sawa et al., RORγt<sup>+</sup> innate lymphoid cells regulate intestinal homeostasis by integrating negative signals from the symbiotic microbiota. *Nat. Immunol.* **12**, 320–326 (2011). doi: [10.1038/ni.2002](https://doi.org/10.1038/ni.2002); pmid: [21336274](https://pubmed.ncbi.nlm.nih.gov/21336274/)
- P. H. Patterson, Immune involvement in schizophrenia and autism: Etiology, pathology and animal models. *Behav. Brain Res.* **204**, 313–321 (2009). doi: [10.1016/j.bbr.2008.12.016](https://doi.org/10.1016/j.bbr.2008.12.016); pmid: [19136031](https://pubmed.ncbi.nlm.nih.gov/19136031/)
- G. Hoeffel et al., C-Myb<sup>+</sup> erythro-myeloid progenitor-derived fetal monocytes give rise to adult tissue-resident macrophages. *Immunity* **42**, 665–678 (2015). doi: [10.1016/j.jimmuni.2015.03.011](https://doi.org/10.1016/j.jimmuni.2015.03.011); pmid: [25902481](https://pubmed.ncbi.nlm.nih.gov/25902481/)
- S. Waksman et al., Developmental neuronal death in hippocampus requires the microglial CD11b integrin and DAPI immunoreceptor. *J. Neurosci.* **28**, 8138–8143 (2008). doi: [10.1523/JNEUROSCI.1006-08.2008](https://doi.org/10.1523/JNEUROSCI.1006-08.2008); pmid: [18685038](https://pubmed.ncbi.nlm.nih.gov/18685038/)
- A. Sierra et al., Microglia shape adult hippocampal neurogenesis through apoptosis-coupled phagocytosis. *Cell Stem Cell* **7**, 483–495 (2010). doi: [10.1016/j.stem.2010.08.014](https://doi.org/10.1016/j.stem.2010.08.014); pmid: [20887954](https://pubmed.ncbi.nlm.nih.gov/20887954/)
- R. C. Paolicelli et al., Synaptic pruning by microglia is necessary for normal brain development. *Science* **333**, 1456–1458 (2011). doi: [10.1126/science.1202529](https://doi.org/10.1126/science.1202529); pmid: [21778362](https://pubmed.ncbi.nlm.nih.gov/21778362/)

28. D. P. Schafer et al., Microglia sculpt postnatal neural circuits in an activity and complement-dependent manner. *Neuron* **74**, 691–705 (2012). doi: 10.1016/j.neuron.2012.03.026; pmid: 22632727
29. D. P. Schafer, E. K. Lehrman, B. Stevens, The “quad-partite” synapse: Microglia-synapse interactions in the developing and mature CNS. *Glia* **61**, 24–36 (2013). doi: 10.1002/glia.22389; pmid: 22829357
30. H. Kettenmann, F. Kirchhoff, A. Verkhratsky, Microglia: New roles for the synaptic stripper. *Neuron* **77**, 10–18 (2013). doi: 10.1016/j.neuron.2012.12.023; pmid: 23312512
31. Y. Zhan et al., Deficient neuron-microglia signaling results in impaired functional brain connectivity and social behavior. *Nat. Neurosci.* **17**, 400–406 (2014). doi: 10.1038/nn.3641; pmid: 24487234
32. A. S. Brown, E. J. Derkets, Prenatal infection and schizophrenia: A review of epidemiologic and translational studies. *Am. J. Psychiatry* **167**, 261–280 (2010). doi: 10.1176/appi.ajp.2009.09030361; pmid: 20123911
33. K. A. Garbett, E. Y. Hsiao, S. Kálmán, P. H. Patterson, K. Mirmics, Effects of maternal immune activation on gene expression patterns in the fetal brain. *Transl. Psychiatry* **2**, e98 (2012). doi: 10.1038/tp.2012.24; pmid: 22832908
34. U. Meyer, J. Feldon, M. Schedlowski, B. K. Yee, Immunological stress at the maternal-fetal interface: A link between neurodevelopment and adult psychopathology. *Brain Behav. Immun.* **20**, 378–388 (2006). doi: 10.1016/j.bbi.2005.11.003; pmid: 16378711
35. U. Meyer et al., The time of prenatal immune challenge determines the specificity of inflammation-mediated brain and behavioral pathology. *J. Neurosci.* **26**, 4752–4762 (2006). doi: 10.1523/JNEUROSCI.0099-06.2006; pmid: 16672647
36. D. Gate, K. Rezai-Zadeh, D. Jodry, A. Rentsendorj, T. Town, Macrophages in Alzheimer’s disease: The blood-borne identity. *J. Neural Transm.* **117**, 961–970 (2010). doi: 10.1007/s00702-010-0422-7; pmid: 20517700
37. C. Prunier, P. H. Howe, Disabled-2 (Dab2) is required for transforming growth factor β-induced epithelial to mesenchymal transition (EMT). *J. Biol. Chem.* **280**, 17540–17548 (2005). doi: 10.1074/jbc.M00974200; pmid: 15734730
38. Materials and methods are available as supplementary materials on Science Online.
39. G. Brady et al., Analysis of gene expression in a complex differentiation hierarchy by global amplification of cDNA from single cells. *Curr. Biol.* **5**, 909–922 (1995). doi: 10.1016/S0960-9822(95)00181-3; pmid: 7583149
40. S. D. J. Calaminus et al., Lineage tracing of Ptf1-Cre marks hematopoietic stem cells and their progeny. *PLOS ONE* **7**, e51361 (2012). doi: 10.1371/journal.pone.0051361; pmid: 23300543
41. I. Amit, D. R. Winter, S. Jung, The role of the local environment and epigenetics in shaping macrophage identity and their effect on tissue homeostasis. *Nat. Immunol.* **17**, 18–25 (2016). doi: 10.1038/ni.3325; pmid: 26681458
42. D. D. Lee, H. S. Seung, Learning the parts of objects by non-negative matrix factorization. *Nature* **401**, 788–791 (1999). doi: 10.1038/44565; pmid: 10548103
43. D. S. Gross, W. T. Garrard, Nuclease hypersensitive sites in chromatin. *Annu. Rev. Biochem.* **57**, 159–197 (1988). doi: 10.1146/annurev.bi.57.071088.001111; pmid: 3052270
44. G. Felsenfeld, M. Groudine, Controlling the double helix. *Nature* **421**, 448–453 (2003). doi: 10.1038/nature01411; pmid: 12540921
45. D. R. Winter, I. Amit, The role of chromatin dynamics in immune cell development. *Immunol. Rev.* **261**, 9–22 (2014). doi: 10.1111/imr.12200; pmid: 25123274
46. J. D. Buenrostro, P. G. Giresi, L. C. Zaba, H. Y. Chang, W. J. Greenleaf, Transposition of native chromatin for fast and sensitive epigenomic profiling of open chromatin, DNA-binding proteins and nucleosome position. *Nat. Methods* **10**, 1213–1218 (2013). doi: 10.1038/nmeth.2688; pmid: 24097267
47. D. Lara-Astiaso et al., Chromatin state dynamics during blood formation. *Science* **345**, 943–949 (2014). doi: 10.1126/science.1256271; pmid: 25103404
48. A. Barski et al., High-resolution profiling of histone methylation in the human genome. *Cell* **129**, 823–837 (2007). doi: 10.1016/j.cell.2007.05.009; pmid: 17512444
49. N. D. Heintzman et al., Distinct and predictive chromatin signatures of transcriptional promoters and enhancers in the human genome. *Nat. Genet.* **39**, 311–318 (2007). doi: 10.1038/ng1966; pmid: 17277777
50. D. A. Jaitin et al., Massively parallel single-cell RNA-seq for marker-free decomposition of tissues into cell types. *Science* **343**, 776–779 (2014). doi: 10.1126/science.1247651; pmid: 24531970
51. F. Paul et al., Transcriptional heterogeneity and lineage commitment in myeloid progenitors. *Cell* **163**, 1663–1677 (2015). doi: 10.1016/j.cell.2015.11.013; pmid: 26627738
52. K. Bahar Halpern et al., Bursty gene expression in the intact mammalian liver. *Mol. Cell* **58**, 147–156 (2015). doi: 10.1016/j.molcel.2015.01.027; pmid: 25728770
53. S. Itzkovitz, I. C. Blat, T. Jacks, H. Clevers, A. van Oudenaarden, Optimality in the development of intestinal crypts. *Cell* **148**, 608–619 (2012). doi: 10.1016/j.cell.2011.12.025; pmid: 22304925
54. A. Lyubimova et al., Single-molecule mRNA detection and counting in mammalian tissue. *Nat. Protoc.* **8**, 1743–1758 (2013). doi: 10.1038/nprot.2013.109; pmid: 23949380
55. E. S. Lein et al., Genome-wide atlas of gene expression in the adult mouse brain. *Nature* **445**, 168–176 (2007). doi: 10.1038/nature05453; pmid: 17151600
56. L. A. Cirillo, K. S. Zaret, An early developmental transcription factor complex that is more stable on nucleosome core particles than on free DNA. *Mol. Cell* **4**, 961–969 (1999). doi: 10.1016/S1097-2765(00)80225-7; pmid: 10635321
57. M. Garber et al., A high-throughput chromatin immunoprecipitation approach reveals principles of dynamic gene regulation in mammals. *Mol. Cell* **47**, 810–822 (2012). doi: 10.1016/j.molcel.2012.07.030; pmid: 22940246
58. A. Aziz, E. Soucie, S. Sarrazin, M. H. Sieweke, MafB/c-Maf deficiency enables self-renewal of differentiated functional macrophages. *Science* **326**, 867–871 (2009). doi: 10.1126/science.1176056; pmid: 19892988
59. L. M. Kelly, U. Englemeier, I. Lafon, M. H. Sieweke, T. Graf, MafB is an inducer of monocytic differentiation. *EMBO J.* **19**, 1987–1997 (2000). doi: 10.1093/emboj/19.9.1987; pmid: 10790365
60. E. L. Soucie et al., Lineage-specific enhancers activate self-renewal genes in macrophages and embryonic stem cells. *Science* **351**, aad5510 (2016). doi: 10.1126/science.aad5510; pmid: 26797145
61. E. Y. Hsiao et al., Microbiota modulate behavioral and physiological abnormalities associated with neurodevelopmental disorders. *Cell* **155**, 1451–1463 (2013). doi: 10.1016/j.cell.2013.11.024; pmid: 24315484
62. L. V. Hooper, D. R. Littman, A. J. Macpherson, Interactions between the microbiota and the immune system. *Science* **336**, 1268–1273 (2012). doi: 10.1126/science.1223490; pmid: 22674334
63. J. E. Koenig et al., Succession of microbial consortia in the developing infant gut microbiome. *Proc. Natl. Acad. Sci. U.S.A.* **108**, 4578–4585 (2011). doi: 10.1073/pnas.1000081107; pmid: 20668239
64. M.-C. Arrieta, L. T. Stiemsma, N. Amenyogbe, E. M. Brown, B. Finlay, The intestinal microbiome in early life: Health and disease. *Front. Immunol.* **5**, 427 (2014). doi: 25250028
65. P. H. Patterson, Maternal infection and immune involvement in autism. *Trends Mol. Med.* **17**, 389–394 (2011). doi: 10.1016/j.molmed.2011.03.001; pmid: 21482187
66. S. Giovanioli, U. Weber-Stadlbauer, M. Schedlowski, U. Meyer, H. Engler, Prenatal immune activation causes hippocampal synaptic deficits in the absence of overt microglia anomalies. *Brain Behav. Immun.* **55**, 25–38 (2015). doi: 10.1016/j.jbbi.2015.09015; pmid: 26408796
67. S. Yona et al., Fate mapping reveals origins and dynamics of monocytes and tissue macrophages under homeostasis. *Immunity* **38**, 79–91 (2013). doi: 10.1016/j.immuni.2012.12.001; pmid: 23273845
68. I. G. Pantano-Feliciano et al., Biphasic assembly of the murine intestinal microbiota during early development. *ISME J.* **7**, 1112–1115 (2013). doi: 10.1038/isme.2013.15; pmid: 23535917
69. K. Baruch et al., Aging-induced type I interferon response at the choroid plexus negatively affects brain function. *Science* **346**, 89–93 (2014). doi: 10.1126/science.1252945; pmid: 25147279
70. Y. Ziv et al., Immune cells contribute to the maintenance of neurogenesis and spatial learning abilities in adulthood. *Nat. Neurosci.* **9**, 268–275 (2006). doi: 10.1038/nn1629; pmid: 16415867
71. N. C. Derecki et al., Regulation of learning and memory by meningeal immunity: A key role for IL-4. *J. Exp. Med.* **207**, 1067–1080 (2010). doi: 10.1084/jem.2009419; pmid: 20439540
72. H. Kim, B. Seed, The transcription factor MafB antagonizes antiviral responses by blocking recruitment of coactivators to the transcription factor IRF3. *Nat. Immunol.* **11**, 743–750 (2010). doi: 10.1038/ni.1897; pmid: 20581830
73. C. J. Nirschl, C. G. Drake, Molecular pathways: Coexpression of immune checkpoint molecules: Signaling pathways and implications for cancer immunotherapy. *Clin. Cancer Res.* **19**, 4917–4924 (2013). doi: 10.1158/1078-0432.CCR-12-1972; pmid: 23868869
74. S. Jung et al., Analysis of fractalkine receptor CX<sub>3</sub>CR1 function by targeted deletion and green fluorescent protein reporter gene insertion. *Mol. Cell. Biol.* **20**, 4106–4114 (2000). doi: 10.1128/MCB.20.1406-4114.2000; pmid: 10805752
75. C. A. Thaiss et al., Transkingdom control of microbiota diurnal oscillations promotes metabolic homeostasis. *Cell* **159**, 514–529 (2014). doi: 10.1016/j.cell.2014.09.048; pmid: 25417104
76. U. Meyer et al., Relative prenatal and postnatal maternal contributions to schizophrenia-related neurochemical dysfunction after *in utero* immune challenge. *Neuropsychopharmacology* **33**, 441–456 (2008). doi: 10.1038/sj.npp.1301413; pmid: 17443130
77. A. Agresti, A survey of exact inference for contingency tables. *Stat. Sci.* **7**, 131–153 (1992). doi: 10.1214/ss/117011454
78. C. Trapnell, L. Pachter, S. L. Salzberg, TopHat: Discovering splice junctions with RNA-seq. *Bioinformatics* **25**, 1105–1111 (2009). doi: 10.1093/bioinformatics/btp120; pmid: 19289445
79. S. Heinz et al., Simple combinations of lineage-determining transcription factors prime cis-regulatory elements required for macrophage and B cell identities. *Mol. Cell* **38**, 576–589 (2010). doi: 10.1016/j.molcel.2010.05.004; pmid: 20513432
80. E. Eden, D. Lipson, S. Yosef, Z. Yakhini, Discovering motifs in ranked lists of DNA sequences. *PLOS Comput. Biol.* **3**, e39 (2007). doi: 10.1371/journal.pcbi.0030039; pmid: 17381235
81. E. Eden, R. Navon, I. Steinfield, D. Lipson, Z. Yakhini, GORilla: A tool for discovery and visualization of enriched GO terms in ranked gene lists. *BMC Bioinformatics* **10**, 48 (2009). doi: 10.1186/1471-2105-10-48; pmid: 19192299
82. S. Picelli et al., TN5 transposase and tagmentation procedures for massively scaled sequencing projects. *Genome Res.* **24**, 2033–2040 (2014). doi: 10.1101/gr.177811.114; pmid: 25079858
83. B. Langmead, C. Trapnell, M. Pop, S. L. Salzberg, Ultrafast and memory-efficient alignment of short DNA sequences to the human genome. *Genome Biol.* **10**, R25 (2009). doi: 10.1186/gb-2009-10-3-r25; pmid: 19261174

**ACKNOWLEDGMENTS**

We thank members of the I.A. and M.S. laboratories for discussions, T. Wiesel for artwork, M. Barad from the CIML flow cytometry platform for assistance with microglia sorting, and M. Azoulay and O. Rozenberg for animal handling. Research in the I.A. laboratory is supported by the European Research Council (grant 309788); the Israeli Science Foundation (grant 1782/11); the European Commission Seventh Framework Programme (EC FP7) BLUEPRINT consortium; the Ernest and Bonnie Beutler Research Program of Excellence in Genomic Medicine; a Minerva Stiftung research grant; the Israeli Ministry of Science, Technology and Space; the David and Fela Shapell Family Foundation; and the National Human Genome Research Institute Center for Excellence in Genome Science (grant IP50HG006193). I.A. holds the Alan and Laraine Fischer Career Development Chair. Research in the M.S. laboratory is supported by the Advanced European Research Council (grant 232835) and by the EC FP7 HEALTH-2011 program (grant 279017). M.S. holds the Maurice and Ilse Katz Professorial Chair in Neuroimmunology. M.H.S. was supported by grants from the Agence Nationale de la Recherche (grants ANR BLAN07-1\_20575 and ANR-11-BSV3-026-01), the Fondation pour la Recherche Médicale (DEq. 20071210559 and DEq. 20101421320), and InCa (French National Cancer Institute; grant 13-10/405/AB-LC-HS). M.H.S. is a Berlin Institute of Health Einstein fellow and an INSERM-Helmholtz group leader. D.R.W. is supported by the European Molecular Biology Organization (EMBO; ALT766-2014) and the EC FP7 (Marie Curie Actions, EMBOCOFUND2012; GA-2012-600394). ATAC-seq, ChIP-seq, bulk RNA-seq, and single-cell RNA-seq data are deposited in the Genome Expression Omnibus under accession number GSE79819.

**SUPPLEMENTARY MATERIALS**

[www.scienmag.org/content/353/aad8670/suppl/DC1](http://www.scienmag.org/content/353/aad8670/suppl/DC1)  
Materials and Methods  
Figs. S1 to S8  
Tables S1 to S10  
14 November 2015; accepted 10 June 2016  
Published online 23 June 2016  
10.1126/science.aad8670

## Microglia development follows a stepwise program to regulate brain homeostasis

Orit Matcovitch-Natan, Deborah R. Winter, Amir Giladi, Stephanie Vargas Aguilar, Amit Spinrad, Sandrine Sarrazin, Hila Ben-Yehuda, Eyal David, Fabiola Zelada González, Pierre Perrin, Hadas Keren-Shaul, Meital Gury, David Lara-Astaiso, Christoph A. Thaiss, Merav Cohen, Keren Bahar Halpern, Kuti Baruch, Aleksandra Deczkowska, Erika Lorenzo-Vivas, Shalev Itzkovitz, Eran Elinav, Michael H. Sieweke, Michal Schwartz and Ido Amit

Science 353 (6301), aad8670.  
DOI: 10.1126/science.aad8670 originally published online June 23, 2016

### Microglia development follows a stepwise program

Microglia are cells that defend the central nervous system. However, because they migrate into the brain during development, the changes that they undergo, including those that affect gene expression, have been difficult to document. Matcovitch-Natan *et al.* transcriptionally profiled gene expression and analyzed epigenetic signatures of microglia at the single-cell level in the early postnatal life of mice. They identified three stages of microglia development, which are characterized by gene expression and linked with chromatin changes, occurring in sync with the developing brain. Furthermore, they showed that the proper development of microglia is affected by the microbiome.

Science, this issue p. 789

#### ARTICLE TOOLS

<http://science.sciencemag.org/content/353/6301/aad8670>

#### SUPPLEMENTARY MATERIALS

<http://science.sciencemag.org/content/suppl/2016/06/22/science.aad8670.DC1>

#### RELATED CONTENT

<http://science.sciencemag.org/content/sci/353/6301/760.full>  
<http://science.sciencemag.org/content/sci/353/6301/762.full>  
<http://science.sciencemag.org/content/sci/353/6301/766.full>  
<http://science.sciencemag.org/content/sci/353/6301/772.full>  
<http://science.sciencemag.org/content/sci/353/6301/777.full>  
<http://science.sciencemag.org/content/sci/353/6301/783.full>

#### REFERENCES

This article cites 82 articles, 20 of which you can access for free  
<http://science.sciencemag.org/content/353/6301/aad8670#BIBL>

#### PERMISSIONS

<http://www.sciencemag.org/help/reprints-and-permissions>

Use of this article is subject to the [Terms of Service](#)

---

Science (print ISSN 0036-8075; online ISSN 1095-9203) is published by the American Association for the Advancement of Science, 1200 New York Avenue NW, Washington, DC 20005. The title *Science* is a registered trademark of AAAS.

Copyright © 2016, American Association for the Advancement of Science